# Influence of Microgroove Dimension on Cell Behavior of Human Gingival Fibroblasts Cultured on Titanium Substrata

Suk Won Lee

The Graduate School
Yonsei University
Department of Dental Science

# Influence of Microgroove Dimension on Cell Behavior of Human Gingival Fibroblasts Cultured on Titanium Substrata

A Dissertation
Submitted to the Department of Dental Science
and the Graduate School of Yonsei University
in partial fulfillment of the
requirements for the degree of
Doctor of Philosophy

Suk Won Lee

June 2007

This certifies that the dissertation of
Suk-Won Lee is approved.

_____
Thesis Supervisor: Keun-Woo Lee

_____
Moon-Kyu Chung

_____
Dong-Hoo Han

_____
In-Chul Rhyu

_____
Won-Yoon Chung

The Graduate School
Yonsei University

June 2007

# 감사의 글

먼 길을 달려오는 동안 마지막까지 어려운 고비마다 깊이 격려해주시고 올바른 길로 이끌어 주신 이근우 지도교수님께 진심으로 감사드립니다. 탁월한 통찰력으로 논문의 틀을 바로잡아주신 정문규 교수님과 날카로운 지적으로 논문의 완성도를 높여주신 한동후 교수님께 깊이 감사드립니다. 본 논문에서 사용된 마이크로그루브에 대한 해박한 지식으로 그 임상적 의미를 일깨워주신 서울치대 치주과학교실의 류인철 교수님과 부족한 제가 세포 실험이 어떠한 것이라는 것을 어렴풋이나마 알게 해주신 구강생물학교실 정원윤 교수님께도 깊은 감사의 마음을 전합니다. 치과의사는 어떻게 살아야 하는지를 몸소 보여주신 이호용 교수님과 본 논문의 아이디어를 처음 접하게 해주신 한종현 교수님께 감사의 말씀을 올립니다. 학창시절 담임 선생님이셨으며 전공 선택을 이끌어주신 강우진 교수님, 언제나 깊은 관심으로 챙겨주시는 문홍석, 심준성 교수님과 지금 이 시각에도 연구에 몰두하고 계실 김선재, 이재훈, 배은경 교수님, 그리고 본 논문에 특히 깊은 관심을 가져주셨던 황선홍 교수님께 자랑스럽게 이 논문을 드리고 싶습니다. 든든한 선배로서, 또한 선배 연구자로서 언제나 질문에 답을 주셨던 인하의대 치과학교실의 오남식 교수님, 시편을 아름답고 신속하게 제작해주신 멤스웨어 조수제 사장님과 윤혜진씨께 감사드립니다. 주말도 반납하며 헌신적으로 실험을 도와주신 성빈센트병원 임상의학연구소 김수연 선생님, 밤이 깊은 줄 모르고 연구에 대한 토론에 응해주셨던 배진완 교수님과 성빈센트병원 동료 교수님들, 그리고 김종수 기공실장님께 역시 감사드립니다.

언제나 깊은 격려로 힘을 주시는 장인어른, 장모님, 올바른 가치관을 심어주시고 삶의 길잡이이신 아버지, 그리고 이 세상에서 나를 가장 사랑해주시는 어머니와 더불어 하나님이 주신 아름다운 선물 혜준이 예준이와 나의 믿음이며 안식처인 사랑하는 아내에게 이 논문을 바칩니다.

2007 년 6 월

저 자 씀

# TABLE OF CONTENTS

# LIST OF FIGURES

# LIST OF TABLES

# ABSTRACT

## Influence of Microgroove Dimension on Cell Behavior of Human Gingival Fibroblasts Cultured on Titanium Substrata

**Suk-Won Lee**, D.D.S., M.S.D.

*Department of Dental Science, Graduate School, Yonsei University*
*(Directed by Prof. Keun-Woo Lee, D.D.S., M.S.D., Ph.D.)*

To enhance interactions between titanium (Ti) oral implants and the surrounding gingival soft tissues, the effects of Ti-surface microgrooves on cell behavior have extensively been investigated. Narrow microgrooves on Ti substrata were verified to induce changes in morphology, cell-substratum adhesion, and gene expression of cultured connective tissue cells, such as fibroblasts. However, their effect on enhancing cell proliferation *in vitro* or on the ability to effectively reduce epithelial down-growth *in vivo*, is not yet clear.

In this study, we hypothesized that surface microgrooves of appropriate depth and extensive width on Ti substrata that enable the cells to readily descend into themselves, would alter various cell behaviors including viability and proliferation of cultured human gingival fibroblasts. For the evaluation, cell adhesion, morphology, viability and proliferation, and gene expression of human gingival fibroblasts cultured on Ti substrata with various dimensions of surface microgrooves were analyzed. The purpose of this study was to determine the dimension of surface microgrooves on Ti substrata that shows the greatest positive influence on characterizing specific cell behavior of cultured human gingival fibroblasts.

Commercially pure Ti discs with surface microgrooves of monotonous

3.5 μm in depth and respective 15, 30, and 60 μm in width were fabricated using photolithography and used as the culture substrata in the three experimental groups in this study (TiD15, TiD30, and TiD60 groups), whereas the smooth Ti disc was used as the control substrata (smooth Ti group). Human gingival fibroblasts were cultured on the four groups of titanium substrata on successive timelines. Cell behaviors, such as adhesion, morphology, viability and proliferation, and gene expression were analyzed and compared between all groups using crystal violet stain, scanning electron microscopy (SEM), XTT assay, and reverse transcriptase-polymerase chain reaction (RT-PCR), respectively. One-way analysis of variance was used in the statistical analyses on the adhesion as well as the viability and proliferation data. From the results of the analyses on various biological activities of human gingival fibroblasts, the following results were obtained.

1. There was no difference between the numbers of human gingival fibroblasts adhered to smooth Ti substrata and those adhered to Ti substrata with surface microgrooves at 1 and 2 h incubation. Fibroblasts merely formed initial cell-substratum contact by the times.
2. In SEM, contact guidance of human gingival fibroblasts parallel to the direction of microgrooves was observed. Cells were able to readily descend into the microgrooves of 30 μm in width and 3.5 μm in depth at the early phase of culture, whereas at the later phase, cells in all groups were found both in the grooves and on the ridges. Cells on the ridge edges or in groove corners were spindle shaped with abundant filopodia formation towards the acid-etched surface inside the microgrooves, thus mimicked the shape of the fibroblasts cultured in three-dimensional (3D) nanoenvironment.
3. On successive timelines, human gingival fibroblasts cultured on Ti substrata with various dimensions of surface microgrooves showed

differences in the rate of reaching their confluence. Human gingival fibroblasts cultured on Ti substrata with microgrooves of 15 µm in width and 3.5 µm in depth significantly increased their viability and proliferation compared with those cultured on smooth Ti substrata after 72 h of culture and decreased after 96 h, whereas the cells on the microgrooves of 30 µm in width and 3.5 µm in depth continued increasing their viability and proliferation up to after 96 h of culture.

4. A joint up-regulation of matrix-assembly genes, such as fibronectin and α5 integrin genes, was noted in human gingival fibroblasts cultured on titanium substrata with microgrooves of 15 and 30 µm in width and an equal 3.5 µm in depth.
5. Gene expression pattern specific to the cells in 3D-matrix culture, such as down-regulation of α-smooth muscle actin gene along with up-regulation of fibronectin and p21 genes, was pronounced in human gingival fibroblasts cultured on Ti substrata with microgrooves of 30 µm in width and 3.5 µm in depth.

In reference to the results above, two conclusions were made.: 1) Surface microgrooves of 15 µm in width and 3.5 µm in depth on titanium substrata increase the viability and proliferation, as well as the expression of genes involved in the matrix assembly of cultured human gingival fibroblasts. 2) Surface microgrooves of 30 µm in width and 3.5 µm in depth on titanium substrata provide human gingival fibroblasts with a three-dimensional context of culture, thus show corresponding gene expression.

---

Key words: Titanium, Microgroove, Fibroblast, Proliferation,
Gene expression

# Influence of Microgroove Dimension on Cell Behavior of Human Gingival Fibroblasts Cultured on Titanium Substrata

*Department of Dental Science,*
*Graduate School, Yonsei University*
*(Directed by Prof. Keun-Woo Lee, D.D.S., M.S.D., Ph.D.)*

**Suk-Won Lee**

## I . INTRODUCTION

Since the establishment of osseointegration as a unique concept in oral implantology, researchers now seek for methods to enhance the interactions between titanium implants and the surrounding soft tissues, known as peri-implant soft tissue reactions. The major class of cells found in peri-implant soft tissues includes gingival fibroblasts whose changes in cell behaviors such as cell-matrix adhesions on microtopographic features have long been the topic of studies done by Brunette[1], Jansen[2], and their coworkers. They suggested that microfabricated grooved surfaces would produce orientation and directed locomotion of epithelial cells *in vitro*, thus inhibit epithelial down-growth on titanium oral implants *in vivo*. Moreover, since surface topography was considered important in establishing connective-tissue organization adjacent to titanium oral implants, fibroblast shape and orientation on such grooved surfaces had extensively been evaluated and the effects of the surface topography of microgrooved titanium substrata on cell behavior *in vitro* and *in vivo* were suggested to depend on the groove dimensions. Among the structures varying in shape and dimension,

microgrooves used in these studies were mainly fabricated from the micromachining technique. In most studies, V-shaped micromachined grooves and their morphologic derivatives were fabricated so as to allow the cell to confront its substratum with defined edges. The degree of cell spreading on such geometry was maximized in two directions. The one, an elongation or a polarization in shape parallel to the long axis of grooves/ridges was considered one of the results from a phenomenon called 'contact guidance', whereas the other, from forming bridges between ridges leading to cell spreading[3]. On sensing such geometry, focal contacts were considered to stiffen[4] and the cellular traction forces exerted through focal contacts increased[5], leading to increased amount of focal adhesions[6]. The adhesion strength even surpassed the amount of externally applied local mechanical force[7,8]. Using focal adhesions as anchors, contractile traction forces exerted by a cell, also called cytoskeletal tension per se or cytoskeletal prestress, together with extracellular matrix (ECM) and cytoskeletal structure were considered to play decisive roles in the control of various biological activities including the gene expression and growth[9]. It has been hypothesized that surface topography could induce direct cell mechanotransduction, thus leads to changes in the probability of gene expression[10]. In these biomechanical models, environments were provided so as to induce changes in cell shape and cell spreading on micropatterned or nanostructured surfaces. Another example would be the strengthened cell adhesions and the resultant increase in traction forces exerted by a cell on sharp edges of microstructures in specific directions[11].

Several studies have reported the induction of the changes in cell shape by microgrooves and these changes were found to be tightly coupled to DNA synthesis and growth in adherent cells[12]. Indeed, human fibroblasts grown on the microgrooved substrata, compared to those on the smooth ones, were significantly elongated and orientated along the grooves leading to an increase in the amount of fibronectin mRNA/cell[13], or displayed alterations in the expression of numerous genes responsible for various biological

activities[14]. However, the induction of the changes in cell shape by microgrooves have mainly been restricted to the use of grooves with several micrometers-wide spacing, which was considered narrower than the diameter of a single human fibroblast. So far, only a few studies compared the proliferating activity of fibroblasts on various dimensions of microgrooves. Majority of these *in vitro* studies used substrata with narrow grooves of 1-10 μm in width, and in contrast to the effective increase in the rate of cell orientation, either the presence of surface microgrooves or groove dimensions were verified to increase the proliferating activity of adhered fibroblasts[15,16,17]. In an *in vivo* attempt to inhibit or reduce the extent of epithelial down-growth using microgrooved implants, contradictory results were reported from the Brunette[18] vs. the Jansen[19] groups. Two differences in the experiment designs were noted between the studies, which were the flexibility of the implanted material and the structural dimension of the parallel microgrooves provided.

Taken together, microgrooves narrower than the diameter of an adhered single fibroblast were considered to induce changes in cell shape leading to increased formation of focal adhesion assembly and alteration in gene expression, but their *in vitro* effect on enhancing cell proliferation or the ability to effectively reduce epithelial down-growth *in vivo* is not yet clear. In this study, we hypothesized that surface microgrooves of appropriate depth and extensive width on titanium substrata that enable the cells to readily descend into themselves, would alter various cell behaviors including proliferation of cultured human gingival fibroblasts. The timeline analysis on the viability and proliferation of fibroblasts cultured on microgrooved Ti substrata has been reported in several studies. However, to our knowledge, gene-expression analysis on the cells in such microenvironment in relation to successive timelines has not been reported so far.

The purpose of this study was to determine an optimal dimension of microgrooves for enhancing cell behavior by analyzing adhesion, morphology, proliferation, and gene expression of human gingival

fibroblasts cultured on titanium substrata with various dimensions of surface microgrooves.

# II . MATERIALS AND METHODS

## A . Cell culture

Healthy gingival tissues were obtained from patients who underwent oral surgery for removing impacted wisdom teeth at St. Vincent's Hospital Department of Dentistry. In all cases, tissues were obtained from subjects following informed consent as prescribed in an approved St. Vincent's Hospital Institutional Review Board (IRB) protocol. Tissues were incubated for 16-22 h in Hank's balanced salt solution (HBSS, Gibco BRL, Grand Island, NY, USA) at 4°C for the purpose of separating connective tissue from epithelium. Obtained connective tissues were cut into small pieces and placed in Petri dishes (direct explant method) in Dulbecco's modified Eagle's medium (DMEM, Gibco BRL, Grand Island, NY, USA) supplemented with penicillin G sodium (50 IU/ml), streptomycin sulfate (50(g/ml), and amphotericin B and were kept overnight at 4°C. Cells or explants were washed 3 times in phosphate-buffered salines (PBS, Gibco BRL, Grand Island, NY, USA) and suspended in DMEM supplemented with 10 % fetal bovine serum (FBS, Sigma-Aldrich Co., St. Louis, MO, USA) and antibiotics. The composition and concentration of the solution were maintained to be used as the culture medium in every experiment in this study (DMEM supplemented with 10% FBS and antibiotics). Suspended fibroblasts were seeded into a T-75 flask (enzymatic dissociation) and incubated in a humidified incubator at 37°C with 5% $CO_2$ in 95% air. When cells reached 80% confluence (about once per week), they were removed and suspended using a trypsin-EDTA solution (0.25% trypsin and 0.1% glucose dissolved in 1 mM of EDTA-saline, Sigma-Aldrich Co., St. Louis, MO, USA), washed, centrifuged and reseeded. The culture medium was changed every second day after seeding. Human gingival fibroblasts with 3rd-4th passage were used in all experiments in this study.

**B . Fabrication of titanium substrata**

A 0.2 mm-thick sheet of commercially pure titanium (Ti) was cut in circles of 10 and 25 mm in diameter to be slightly greater in area compared to the floors of the 96- and 24-well tissue culture plates, respectively. The prepared Ti discs were washed and dried in acetone, mechanically polished to obtain a finish surface with Ra ≤ 0.15 μm, and used as the culture substrata in the control groups, smooth Ti, in this study. The finish surface was created so as to mimic the surfaces of the trans-gingival areas of commercially available Ti dental implant abutments. The Ti substrata used in other experimental groups were fabricated with photolithography (MEMSware Inc., Gyoenggi, Kwangju, Korea). In brief, the mechanically polished smooth Ti discs were coated with a UV-sensitive polymer (photo-resist, DTFR, Dongjin, Seoul, Korea). The coated surfaces were exposed to ultraviolet (UV) light through a patterned photo-mask to develop the initial micropatterns. The photo-mask presented the geometric feature of continuously repeated micropatterns of various dimensions. The mask was made of a quartz plate selectively coated with a thin layer of non-transparent chromium to create light-accessible windows. The design of the mask was previously created with computer-aided design (CAD) software. Future grooves were designed to have an equal depth of 3.5 μm and widths of 15, 30, and 60 μm, respectively. The widths of the automatically created ridges were identical to those of the grooves. A monotonous depth of 3.5 μm was chosen because with photolithography, it was the greatest depth available coupled with 15 μm-wide grooves. The micropatterns were developed by immersing the coated Ti discs in a solvent (2.38% tetra-methyl-ammonium-hydroxide, TMAH, Dongjin, Seoul, Korea) that only dissolves the exposed areas. Grooves were created by the micropatterns etched into the mechanically polished smooth Ti surfaces with 1% hydrofluoric acid (HF) and the residual photo-resist coatings were removed in a solvent (acetone and isopropyl-alcohol) (Fig. 1). The fabricated surfaces of the Ti substrata

with microgrooves of 15 and 30 μm in width and monotonous depth of 3.5 μm are shown in Fig. 2. The nomenclature for the structures is based on the dimensions of groove width only, and the depth was not included. For example, if the groove width of the Ti disc/substratum was 30 μm and the depth was 3.5 μm, it was termed TiD30. In all experiments, fabricated Ti substrata were cleaned 3 times in an ultra-sonic device for 30 minutes, washed 3 times in distilled water, left in 20 % ethanol for 10 min, and washed another 5 times before plating the cells.

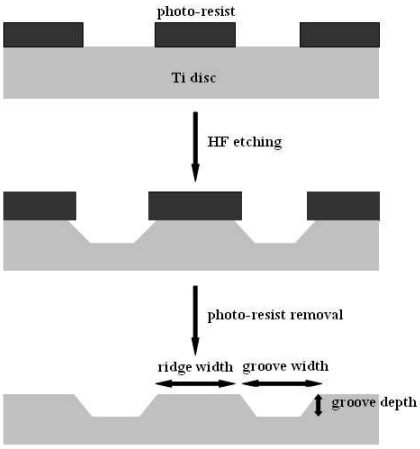


Fig. 1. Fabrication of Ti substrata using photolithography. Note that definitions of the microstructural dimensions are indicated. The microstructural dimensions were included in nomenclature used in this study.

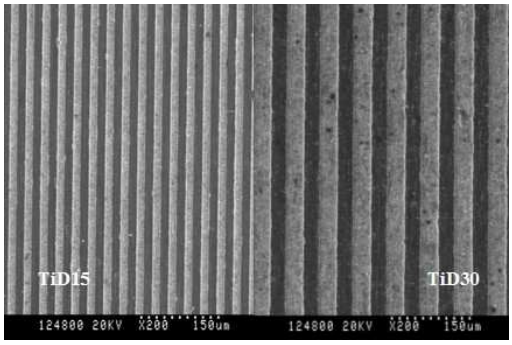


Fig. 2. Fabricated surfaces of the Ti substrata with microgrooves of 15 μm (left) and 30 μm (right) in width and monotonous depth of 3.5 μm.

## C . Adhesion assay

The floors of 96-well plates were removed and the remaining plastic cylinders were attached to the fabricated surfaces of the 10 mm-diameter Ti discs using a silicone bonding agent. As a result, a total of twenty four 96-well Ti substrata were prepared and divided into the four groups of smooth Ti, TiD15, TiD30, and TiD60. Cultured human gingival fibroblasts (3rd-4th passage) were detached from subculture with trypsin-EDTA, resuspended, and plated simultaneously on the 96-well Ti substrata at a cell population density of $3 \times 10^3$ cells/ml in DMEM supplemented with 10% FBS and antibiotics. From three samples out of six in each group, the media were removed at respective 1 and 2 h incubation and the unattached cells were washed away twice with warmed PBS. Attached cells were stained with a solution of 0.2 % crystal violet in 10 % ethanol for 5 min at room temperature. Stained cells were washed with PBS and the bound dye was solubilized with 100 μl of solubilization buffer (50/50 mixture of 0.1 M $NaH_2PO_4$, Ph 4.5 and 50 % ethanol) to be transferred to 96-well plates. Absorbance (optical density, OD) was measured using ELISA analyzer (Spectra MAX 250, Molecular Devices Co., Sunnyvale, CA, USA) at 570 nm.

## D . Scanning electron microscopy

Adhesion and morphology of fibroblasts on the surfaces of fabricated Ti substrata of smooth Ti, TiD15, TiD30, and TiD60 was analyzed under scanning electron microscopic (SEM) observations. At 16 and 48 h plating and incubation, samples were fixed in 4% paraformaldehyde for 2 h and rinsed twice in 0.1*M* PBS for 10 min. Samples were again fixed for another 2 h in 1% osmium tetroxide. Samples were then dehydrated by immersing for 10 min in each of 20, 50, 60, 70, 80, 90, and 100% ethanol dilutions followed by drying with a critical point dryer (Jumb, Bio-Rad Laboratories

Inc., Hercules, CA, USA). Samples were sputter coated with a 10-nm gold film (SEM coating system, E 5150, Bio-Rad Laboratories Inc., Hercules, CA, USA) and imaged with S-800 FE-SEM® (HITACHI, Tokyo, Japan).

**E . XTT assay**

A total of forty eight 24-well Ti substrata were prepared and divided into the four groups of smooth Ti, TiD15, TiD30, and TiD60. Cultured human gingival fibroblasts were trypsinized and simultaneously plated on the 24-well Ti substrata at a cell population density of $1 \times 10^4$ cells/ml in DMEM supplemented with 10% FBS and antibiotics. Cells were incubated in a humidified incubator at 37°C with 5% $CO_2$ in 95% air for 24, 48, 72, and 96 h. In all groups, the viability and proliferation of fibroblasts was determined by XTT assay (Cell Proliferation Kit II, Roche Applied Science, Mannheim, Germany) as described by Roehm *et al.*[20] (1991). In brief, XTT labeling reagent (soium 3'-[1-[(phenylamino)-carbonyl]-3, 4-tetrazolium]-bis(4-methoxy-6- nitro)benzene-sulfonic acid hydrate) and electron coupling reagent (N-methyl dibenzopyrazine methyl sulfate, PMS in PBS) were thawed. Each vial was thoroughly mixed and a clear solution was obtained. XTT labeling mixture was prepared by mixing 50 μl of XTT labeling reagent and 1 μl of electron coupling reagent. 50 μl of XTT labeling mixture was added per well and incubated for 4 h in a humidified incubator at 37°C with 5% $CO_2$ in 95% air. In all groups, formazan products were transferred to 96-well plates and the absorbance was measured using ELISA analyzer (Spectra MAX 250, Molecular Devices Co., Sunnyvale, CA, USA) at 470 nm with a reference wavelength at 650 nm.

**F . RT-PCR**

Fibroblasts were trypsinized at 24, 48, 72, and 96 h incubation. Gene expression of human gingival fibroblasts cultured on the untreated floors of

24-well polystyrene microplates served as the positive control. Total RNA in each sample was extracted using Trizol (Trizol: U.S. Patent No. 5, 346,994, Gibco BRL, Grand Island, NY, USA) according to the manufacturer's instructions. The concentration of extracted total RNA in each sample was estimated by the absorption at 260nm. 1 mg of total RNA samples was converted to cDNA with reverse transcriptase (Promega Co., Madison, Wisconsin, USA). The polymerase chain reaction was carried out using Taq polymerase (Roche Diagnostics, Mannheim, Germany), 10 x buffer, 25mM $MgCl_2$ and 25mM dNTPs (dGTP, dCTP, dATP and dTTP). Expression of various genes involved in cell-matrix adhesion and cell-cycle progression were analyzed in reverse transcriptase-polymerase chain reaction (RT-PCR) (Table 1). The PCR primer of β-actin was used as the housekeeping gene. The amplification was done in a PCR thermal cycler (Bio-Rad Laboratories Inc., Hercules, CA, USA) under the following conditions: 35 cycles of 94 ℃ for 30 sec, 58 ℃ for 45 sec, and 72 ℃ for 30 sec. The amplification products were electrophoresed on 2% agarose gels, and visualized with ethidium bromide. The density of each mRNA was compared using quantitative analysis software (Bio-Rad Laboratories Inc., Hercules, CA, USA) between the groups on successive timelines.

**G . Statistical analysis**

Experiments were repeated simultaneously and independently in triplicate. The mean values and standard deviations of the data from the adhesion and XTT assay were calculated. One-way analysis of variance (ANOVA) in SPSS 13.0 software program was used to compare the mean values of the data between the groups of smooth Ti, TiD15, TiD30, and TiD60 ($p<0.05$).

Table 1. Gene-Specific Primers used in RT-PCR

| Target | Sense | Antisense | Bp |
|---|---|---|---|
| FN[21] | 5'-CGAAATCACAGCCAGTAG-3' | 5'-ATCACATCCACACGGTAG-3' | 639 |
| α5 integrin[22] | 5'-ACCAAGGCCCCAGCTCCATTAG-3' | 5'-GCCTCACACTGCAGGCTAAATG-3' | 376 |
| β1 integrin[23] | 5'-GAGCAGCAAGGACTTTGGG-3' | 5'-GAGCAGCAAGGACTTTGGG-3' | 537 |
| cyclin D1[24] | 5'-ATTAGTTTACCTGGACCCAG-3' | 5'-GATGGAGCCGTCGGTGTAGATGCA-3' | 399 |
| cyclin E[25] | 5'-CAGCCTTGGGACAATAATGC-3' | 5'-TGCAGAAGAGGGTGTTGCTC-3' | 254 |
| cyclin A2[24] | 5'-ATTAGTTTACCTGGACCCAG-3' | 5'-CACAAACTCTGCTACTTCTG-3' | 443 |
| CDK4[26] | 5'-CCAAAGTCAGCCAGCTTGACTGTT-3' | 5'-CATGTAGACCAGGACCTAAGGACA-3' | 193 |
| CDK6[26] | 5'-TGATGTGTGCACAGTGTCACGAAC-3' | 5'-CTGTATTCAGCTCCGAGGTGTTCT-3' | 737 |
| CDK2[26] | 5'-ACGTACGGAGTTGTGTACAAAGCC-3' | 5'-GCTAGTCCAAAGTCTGCTAGCTTG-3' | 405 |
| p21[26] | 5'-AGTGGACAGCGAGCAGCTGA-3' | 5'-TAGAAATCTGTCATGCTGGTCTG-3' | 380 |
| p27[26] | 5'-AAACGTGCGAGTGTCTAACGGGA-3' | 5'-CGCTTCCTTATTCCTGCGCATTG-3' | 454 |
| Skp2[27] | 5'-CAACTACCTCCAACACCTATC-3' | 5'-TCCTGCCTATTTTCCCTGTTCT-3' | 326 |
| α-SMA[28] | 5'-GTCCACCGCAAATGCTTCTAA-3' | 5'-AAAACACATTAACGAGTCAG-3' | 141 |
| TGF-βR-I[29] | 5'-ATTGCTGGACCAGTGTGCTTCGTC-3' | 5'-TAAGTCTGCAATACAGCAAGTTCCATTCTT-3' | 668 |
| TGF-βR-II[29] | 5'-CGCTTTGCTGAGGTCTATAAGGCC-3' | 5'-GATATTGGAGCTCTTGAGGTCCCT-3' | 395 |
| NF-κB1[30] | 5'-CCTGGATGACTCTTGGGAAA-3' | 5'-CTAGCCAGCTGTTTCATGTC-3' | 174 |
| β-actin | 5'-ATCGTGGGCCGCCCTAGGCA-3' | 5'-TGGCCTTAGGGTTCAGAGGGG-3' | 345 |

FN: fibronectin, CDK: cyclin-dependent kinase, p21: cyclin-dependent kinase inhibitor 1A, p27: cyclin-dependent kinase inhibitor 1B, Skp2: S-phase kinase-associated protein-2, α-SMA: α-smooth muscle actin, TGF-βR-I: type I transforming growth factor (TGF-)β receptor, TGF-βR-II: type II transforming growth factor (TGF-)β receptor, NF-κB1: nuclear factor of kappa light polypeptide gene enhancer in B-cells 1

# III . RESULTS

## A . Adhesion analysis

In ANOVA, the mean OD values from the adhesion assay at 1 and 2 h incubation showed no significant differences between and within all groups ($p<0.05$) (Table 2 and Fig. 3).

Table 2. Comparison of fibroblast adhesion to Ti substrata at 1 and 2 h incubation by structural dimensions of surface microgrooves.

| | Ti substrata with various dimensions of surface microgrooves | | | | p-value[1)] |
|---|---|---|---|---|---|
| | Smooth Ti | TiD15 | TiD30 | TiD60 | |
| | n = 3 | n = 3 | n = 3 | n = 3 | |
| 1 h | 0.082±0.007 | 0.102±0.011 | 0.096±0.020 | 0.107±0.016 | ns 0.244 |
| 2 h | 0.134±0.029 | 0.127±0.023 | 0.135±0.030 | 0.147±0.039 | ns 0.879 |

1) Statistical significances were tested by one-way analysis of variance among groups.
TiD: titanium Disc

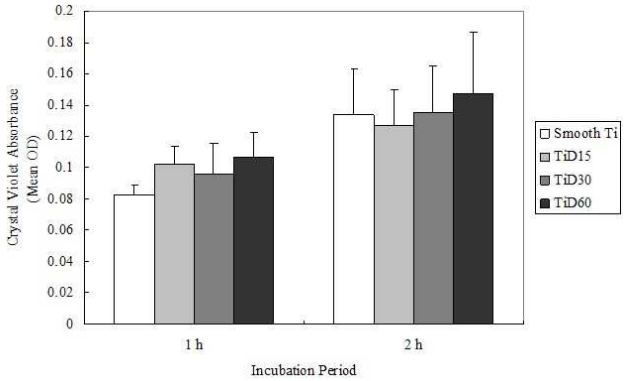


Fig. 3. Effect of structural dimensions of surface microgrooves on human gingival fibroblast adhesion to Ti substrata.

The mean optical density (OD) values and standard deviations of crystal violet absorbance are presented.

$p<0.05$, OD: optical density, TiD: titanium disc

**B . Morphological analysis**

In SEM, orientation of fibroblasts along the microgrooves on TiD15, TiD30, and TiD60 were observed at 16 h incubation, whereas the cells on the smooth Ti were observed to be oriented in random directions (Fig. 4). At 48 h, more extensive orientations on TiD15, TiD30, and TiD60 were observed (Fig. 5). On both timelines, the degree of fibroblast alignment according to the orientation angle in relation to the direction of the microgrooves was not significantly different between TiD15, TiD30, and TiD60. Fibroblasts on the smooth Ti substrata were extensively spread and showed a flat morphology. In contrast, fibroblasts on microgrooved Ti substrata were elongated and less flat compared to those on smooth Ti substrata. (Fig. 6) General morphology of the cells did not vary with the groove dimensions. On all microgrooved Ti substrata, cells were present inside the microgrooves as well as outside on the ridges with a difference in the tendency between 16 and 48 h. Cells were generally observed to be present on the ridges rather than inside the grooves at 16 h, whereas at 48 h, cells were observed both on the ridges and in the grooves (Fig. 7). Notably, majority of the cells were found inside the grooves on TiD30 both at 16 and 48 h (Fig. 7). In all groups, the entire surfaces of the substrata were filled up with fibroblasts at 48 h, suggesting that fibroblasts almost reached their confluence, except in TiD15 where relatively fewer cells were found inside the grooves compared with those in the ridges. Cells descending into the grooves were generally found on the edges or in the corners of the microstructures. These cells showed well elongated spindle shape and increased formation of filopodia (Fig. 8). Numerous filopodia from the cells lying across the borders between ridges and grooves projected towards the acid-etched surfaces inside the grooves, with some extending in a range of tens of micrometers (arrows in Fig. 9), suggesting that these cells were actively exploring the surfaces (Fig. 9). The diameter of a spindle-shaped single fibroblast appeared to be identical to that of the microgrooves in TiD15.

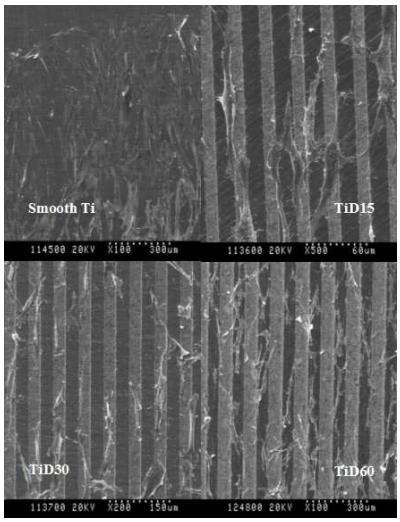


Fig. 4. Scanning electron microscopic (SEM) observations on human gingival fibroblast morphology and orientation at 16 h of culture. Note that the cells are aligned in random directions on smooth Ti substrata. Contact guidance is observed in cells cultured on microgrooved Ti substrata.

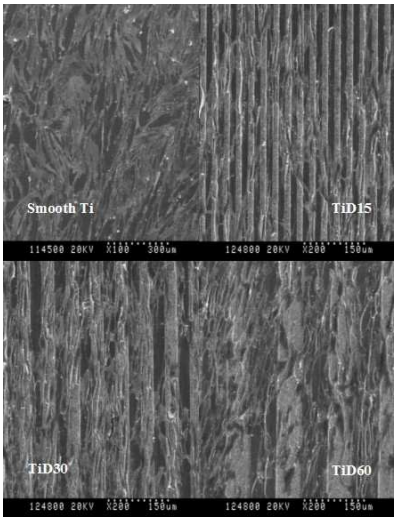


Fig. 5. Scanning electron microscopic (SEM) observations on human gingival fibroblast morphology and orientation at 48 h of culture. Note that the cells are more oriented parallel to the microgrooves than the cells at 16 h of culture.

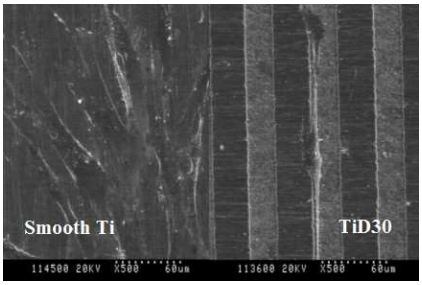


Fig. 6. Scanning electron microscopic (SEM) observations on human gingival fibroblast morphology at 16 h of culture in higher magnification (x 500). The cells on smooth Ti substrata show extremely flattened morphology, whereas the cells on grooved substrata show elongation parallel to the groove direction

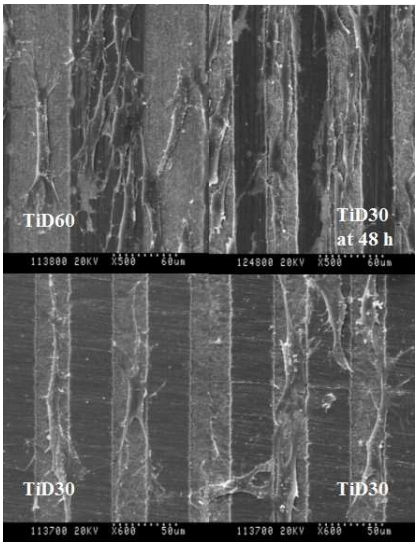


Fig. 7. Scanning electron microscopic (SEM) observations on human gingival fibroblast morphology at 16 and 48 h of culture. Cells were generally observed to be present on the ridges compared to those inside the grooves at 16 h (upper left), whereas at 48 h, cells were observed both on the ridges and in the grooves (upper right). However, majority of the cells were found inside the grooves on Ti substrata with microgrooves of 30 μm in width at both 16 and 48 h of culture.

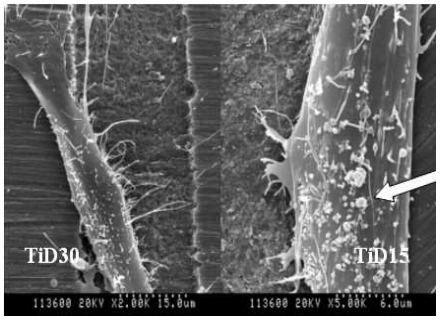


Fig. 8. Scanning electron microscopic (SEM) observations on human gingival fibroblast lying on the edge at 16 h of culture. Note that cells show well elongated spindle shape with abundant filopodia projections toward the acid-etched surface inside the microgrooves. Dot-like projections indicated by the arrow imply that the cells are highly viable.

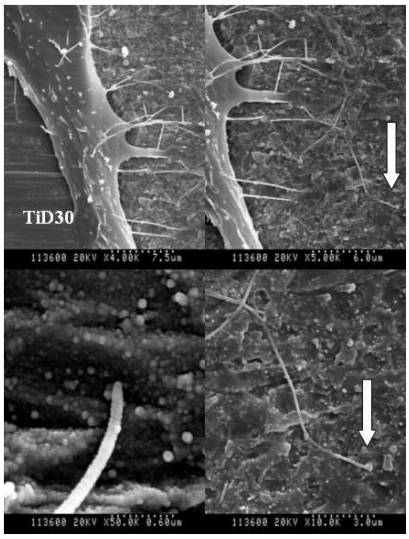


Fig. 9. Scanning electron microscopic (SEM) observations on human gingival fibroblast with abundant filopodia projections at 16 h of culture. The filopodium indicated by the arrow is extended in a range of tens of micrometers, suggesting that these cells are actively exploring the surface.

## C . Assessment of viability and proliferation

In ANOVA, the mean OD values of the formazan absorbance at 72 h incubation were significantly different between and within all groups ($p<0.05$). According to the data using the Ti discs with various dimensions of surface microgrooves as culture substrata, the results from the XTT assay were significantly related between those obtained at 72 h incubation. Multiple comparison of the fibroblast viability and proliferation data from the XTT assay at 72 h incubation showed the mean OD value of TiD15 was significantly greater compared to that of the control group, smooth Ti ($p<0.05$) (Table 3 and Fig. 10). All other comparisons between groups were not statistically significant. As was noted in the timeline analysis, the mean OD value in TiD15 continuously increased up to 72 h, with a burst of increase between the time points of 48 and 72 h, but markedly decreased at 96 h. However, the mean OD values in the groups of smooth Ti and TiD30 continuously increased up to 96 h, with the latter showing slightly higher rate of increase.

Table 3. Comparison of fibroblast viability and proliferation on Ti substrata after 24, 48, 72, and 96 h of culture by structural dimensions of surface microgrooves.

| | Ti substrata with various dimensions of surface microgrooves | | | | |
|---|---|---|---|---|---|
| | Smooth Ti | TiD15 | TiD30 | TiD60 | p-value[1)] |
| | n = 3 | n = 3 | n = 3 | n = 3 | |
| 24 h | 0.310±0.010 | 0.294±0.047 | 0.343±0.030 | 0.327±0.043 | ns 0.417 |
| 48 h | 0.439±0.050 | 0.471±0.058 | 0.492±0.005 | 0.460±0.022 | ns 0.472 |
| 72 h | 0.513±0.063 | 0.795±0.143 | 0.636±0.080 | 0.561±0.107 | < 0.05 |
| T[2)] | a | b | a,b | a,b | |
| 96 h | 0.586±0.103 | 0.586±0.163 | 0.718±0.082 | 0.566±0.024 | ns 0.328 |

1) Statistical significances were tested by one-way analysis of variance among groups.

2) The same letters indicate non-significant difference between groups based on Tukey's multiple comparison tests.

TiD: Titanium Disc

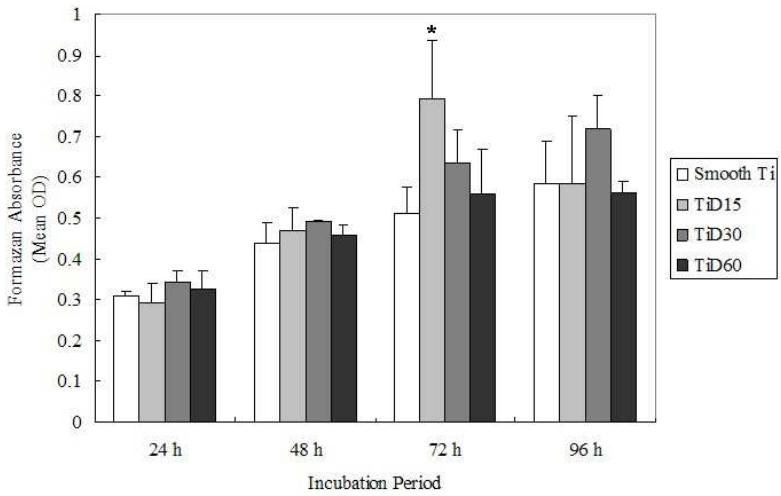


Fig. 10. Effect of structural dimensions of surface microgrooves on human gingival fibroblast viability and proliferation on Ti substrata.

The mean optical density (OD) values and standard deviations of formazan absorbance are presented.

*: Significantly greater compared with the smooth Ti (control) group

$p<0.05$, OD: optical density, TiD: titanium disc

**D . Gene expression analysis**

Increased levels of expression of transcripts in TiD15 and TiD30 were noted with the genes encoding FN, α5 integrin, β1 integrin, cyclin E, CDK2, and CDK4 at 24, 48, and 72 h incubation compared with those in the groups of polystyrene and smooth Ti. On the other hand, decrease in cyclin D1, cyclin A2, and α-SMA gene expression levels were noted in TiD15 and TiD30 on all timelines compared with those in the groups of polystyrene and smooth Ti. In comparison between groups on successive timelines of culture, CDK6, p21, p27, Skp2, TGF-βR-I, TGF-βR-II, and NF-κB1 genes showed controversial results in the expression levels (Fig. 11).

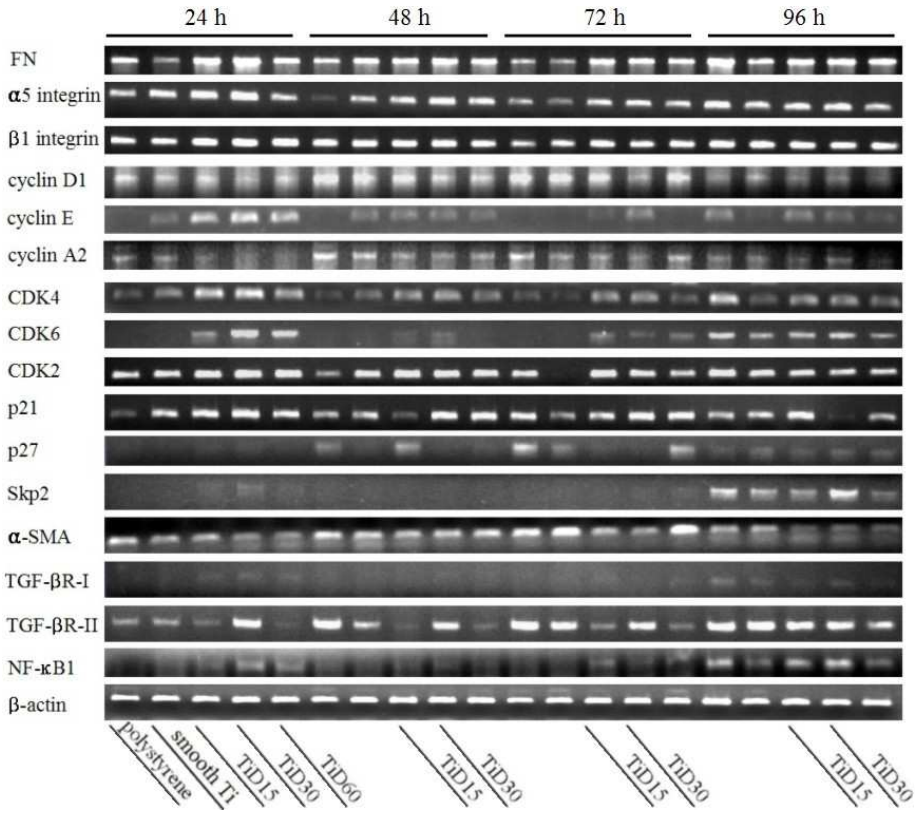


Fig. 11. Analysis on expression of genes involved in cell-matrix adhesion and G1/S cell cycle progression in RT-PCR.

TiD: titanium disc, RT-PCR: reverse transcriptase-polymerase chain reaction FN: fibronectin, CDK: cyclin-dependent kinase, p21: cyclin-dependent kinase inhibitor 1A, p27: cyclin-dependent kinase inhibitor 1B, Skp2: S-phase kinase-associated protein-2, α-SMA: α-smooth muscle actin, TGF-βR-I: type I transforming growth factor (TGF-)β receptor, TGF-βR-II: type II transforming growth factor (TGF-)β receptor, NF-κB1: nuclear factor of kappa light polypeptide gene enhancer in B-cells 1

# IV . DISCUSSION

From previous studies it is known that fibroblasts need less than 4 h for adapting their morphology to a new environment[31]. Therefore experiment times for the adhesion assay were chosen of 1 and 2 h, which were less than 4 h. During this time, adhered fibroblasts to Ti substrata with different surface topographies were expected to show differences in number. Since the unattached cells were washed away, only the remaining adhered fibroblasts were considered to be stained with crystal violet. Measuring the optical density value of the dye would represent the number of adhered cells. The result showed that surface microgrooves on Ti substrata were not able to enhance cell-substratum adhesion of human gingival fibroblasts at 1 and 2 h incubation after plating. This is partly in line with the result from a previous study that fibroblast attachment to microgrooved substrates decreased at the early time points but drastically increased at later phases[32]. The authors observed in SEM images that 30 min after plating, cells already formed abundant membrane extensions. They expected that the cells were then in the process of exploring and probing the surface. However, the culture substrates they used were microgrooved polystyrene tissue culture dishes with a radio-frequent glow discharge treatment to improve the surface wettability of the substrates, which do not coincide with the substrates used in our study. Let alone the use of such special treatment, it is known that commercially available cell culture plates consist of the high-grade polystyrene subsequently treated to create a surface hydrophilicity which is necessary for cell attachment and spreading[33]. During the incubation periods, we observed the cells simultaneously plated on the polystyrene surfaces in light microscopy and confirmed that fibroblasts were not yet spread at 1 h incubation but were starting to at 2 h. In case of microgrooved substrata, cellular spreading is associated with a rapid orientation parallel to the surface grooves. Oakley *et al.*[34] (1997) observed that human gingival fibroblasts

generally spread radially across the ridges and grooves and gradually elongate in a direction parallel to the grooves within 6 h of seeding. However, the difference in the degree of alignment between 15- and 3-µm to 5-µm grooves diminished at 24 h. Results from the separate studies, including the one from ours, suggest that elongated and aligned fibroblasts on microgrooved substrata would start to show increased adhesion, compared to those on smooth substrata, at a specific time point from 4 to 6 h. Our result from the adhesion assay at 1 and 2 h incubation strongly implies that primary human gingival fibroblasts were not capable of forming cell-substratum adhesion, but merely formed the initial cell-substratum contact to the surfaces of Ti substrata on the experimental timelines.

In natural tissues, gingival fibroblasts are arranged in a three-dimensional (3D) organization that provides appropriate functional and spatial conditions. To mimic this environmental characteristic of natural tissues *in vitro*, we prepared the Ti substrata with surface microgrooves of reasonable width and depth. The dimensions of the microstructures used in this study were designed to be ensured that human gingival fibroblasts would, at the same, lie inside the grooves and display contact guidance[35]. To verify this, we plated fibroblasts at a cell population density of $1 \times 10^3$ cells/ml and observed at 16 and 48 h incubation. The plated cell number was selected so as to inhibit intercellular collision. 16 h was selected according to the studies demonstrating that, on both materials of Ti and polyacrylamide, fibroblasts deposit sufficient amount of fibronectin (FN) onto the substrates for cell-matrix adhesion by the time point[13,36]. Deposition of FN by the cells was considered to enable them to form cell-matrix adhesions leading to subsequent spreading or elongation. In SEM, majority of the typical spindle-shaped fibroblasts were found on ridge edges or in groove corners. Filopodia formation was abundant in these cells as has previously been reported[37]. Also abundant were the small dot-like protrusions on cell dorsa which were considered to be metabolite-secreting vesicles or filopodia budding (arrow in Fig. 8). Fibroblasts featuring abovementioned characteristics in SEM images

were considered to be highly viable and very similar in overall shape to those of fibroblasts cultured in 3-D nanoenvironment[38,39]. The observed filopodia mainly projected towards the acid-etched surfaces of the grooves, implying that these cells were actively exploring the surfaces before migrating (arrows in Fig. 9). This result supports other results from two very recent studies demonstrating the importance of filopodia in cell behavior. A study by Partridge and Marcantonio[40] (2006) verified that filopodia containing both integrin and actin formed the initial cell-matrix contacts and further generated mature focal adhesions. Another recent study by Galbraith et al.[41] (2007) suggested that actin and β1 integrin in cellular projections including filopodia at the leading edge of a migrating cell, probe ligand and create sticky fingers. Since fibroblasts are the most abundant cells found in gingival connective tissues, active projection of filopodia onto the acid-etched surfaces inside the microgrooves observed in this study encourages the use of such surface in enhancing peri-implant connective tissue attachment[42].

One of the most frequently used colorimetric assays, XTT, used in this study is a method well established in investigating the influence of a specific substance/material and/or process on cell survival. The results of the XTT assay for cell viability and proliferation are influenced not only by the number but also by the metabolic activity of cells. Cleavage of XTT by dehydrogenase enzymes of metabolically active cells yields a highly colored formazan product which is water soluble. This feature enables the product to be diluted in medium, eliminates the need for formazan crystal solubilization prior to absorbance measurements as is required in MTT assay, protects cellular membranes from being damaged, and leads the cells to survive throughout the test process[20]. On planning for this experiment, we expected the fibroblasts to show increased proliferation on the microgrooved Ti substrata compared with the smooth ones. The results from the timeline proliferation analysis using XTT assay gave us no reason to confirm such expectation except the result, at 72 h incubation, that fibroblasts in TiD15

showed a burst of increase in proliferation, but suddenly decreased on the successive timeline at 96 h. This, in part, corresponds with the results in the study by Dalby *et al.*[14] (2003) that on the quartz substrata with surface microgrooves of 12.5 µm in width, fibroblasts showed up-regulation of genes involved in cell signaling, DNA transcription, RNA-protein translation, and extracellular matrix formation and remodeling after 24 h of culture, while all the genes were down-regulated by day 5. They suggested two reasons for this unique result. First, cell types of mesenchymal origin are highly proliferative initially (Days 0–3), and then, as confluence is approached, this proliferation slows and the cells start to differentiate and produce matrix, ultimately making new tissue. This is also true with the time–line of cultured cells' proliferation in microenvironments[43]. Fibroblasts on both TiD15 were considered to have reached confluence at a certain time point around 72 h of culture. We suggest that human gingival fibroblasts cultured on Ti substrata with surface microgrooves of 15 µm in width and 3.5 µm in depth reach their confluence earlier compared with those cultured on the smooth Ti or Ti substrata with greater dimensions of surface microgrooves. The second reason suggested by Dalby[14] (2003) and his coworkers was that as the cells align in response to the grooves, cell activities are initially increased and thus take on far less random morphologies than are produced on the flat surfaces. The nuclei shapes would be restricted leading to the restriction of chromosomal arrangement and result in the down-regulation at later phases. This suggestion does not coincide with our results from the morphologic analysis that, in SEM at 48 h, the majority of fibroblasts were still observed to be incapable of moving into the grooves of 15 µm in width. It seems unlikely that any of the fibroblasts cultured in our experiment would have experienced such nucleic deformation. In TiD30 however, a gradual increase in proliferating activities was noted on successive timelines up to 96 h.

Since proliferating data of the cells cultured on substrata with relatively greater microgrooves in dimension are so scarce, we found a somewhat

corresponding result from a very recent study analyzing on microgroove-related cell migration and alignment[44]. They used 3T3 fibroblastic cells plated on structured Ti-alloy surfaces with groove depth/ridge height of 5-22 µm, and spacing of 5-30 µm. Cells migrating on surface structures with groove or ridge width up to 20-30 µm exhibited the highest mean migration velocity. Similar to our findings in SEM, the authors found no significant difference in the frequencies of a certain type of cell shape among the surface structures with different dimensions. Also, they strongly implied that the width of 30 µm roughly represents the main diameter of the cells. This also corresponds with our SEM findings that at 16 h incubation, compared with the results at 48 h, only the fibroblasts on TiD30 substrata were generally found inside the grooves compared with other grooves, and that, a single cell in one groove. The importance of the presence of cell contact on the bottom of the grooves in relation to contact guidance in mechanical point of view has been suggested by Walboomers *et al.*[17] (1999). The authors also concluded that at confluence, microgrooves with relatively wider grooves of 20 µm in width compared to the narrower ones were able to support greater numbers of cells. In the groups of smooth Ti and TiD60, fibroblasts showed no more increase in viability and proliferation at 96 h compared to that at 72 h, implying that they were or, at least, were about to reach their confluence at around 72 h. However, a continuous increase was seen in TiD30 even at 96 h, suggesting that the fibroblasts were still proliferating at the time. Indeed, in a study using polymethylmethacrylate (PMMA) surfaces with precise 3D microgrooved structures, wider and deeper grooves of 30 µm in width and 20 µm in depth mostly stimulated fibroblast proliferation[45]. Taken together, we suggest that microgrooves of 30 µm in width enable human gingival fibroblasts to readily descend into the grooves in early phases of culture, thus lead the cells to proliferate for longer period of time, but this suggestion leaves much to be investigated using appropriate methods to analyze the differences in the rate of cell proliferation. Once the cells lie in a groove, the probability of protrusion attachment outside the groove becomes small due

to the convex character of the groove edge[46]. Since microgrooves have been verified to influence the deposition patterns of ECM proteins[47] and the ECM guides the orientation of the cell division axis[48], proliferation of the cells lying in a groove would be influenced by the dimension of the structure.

In this study, the purpose of using both adhesion and XTT assay was twofold: 1) to assay the cell-substratum adhesion and proliferation of fibroblasts plated on titanium substrata with different dimensions of microgrooves and 2) to determine, after plating, the optimal time period of incubation at which fibroblasts on the microgrooved Ti substrata would show significantly greater extent of viability and proliferation compared with those on smooth Ti substrata. It was under the verifications of the abovementioned conditions that expression of genes related to cell-substratum adhesion and adhesion-dependent cell cycle progression of plated fibroblasts were analyzed in RT-PCR. However, we statistically failed to verify the specific timeline as well as dimension of microgrooves on which human gingival fibroblasts would show enhanced both cell-substratum adhesion and viability/proliferation compared to those in other experimental conditions. For most types of cells, the opportunities for anchorage and attachment depend on the surrounding matrix, which is usually made by the cell itself. Thus, a cell can create an environment that then acts back on the cell to reinforce its differentiated state. Furthermore, the ECM that a cell secretes forms part of the environment for its neighbors as well as for the cell itself, and thus tends to make neighboring cells differentiate in the same way, which in another term, contact guidance[49]. Fibroblasts also need adhesions to the ECM for their proliferation and growth. Fibroblasts undergo cell spreading on adhesion to the ECM such as FN fibrils. In the event, the generated forces by the cells align and stiffen ECM and partially unfold ECM proteins[50]. Up-regulation of FN gene in TiD15 and TiD30 at 24 and 72 h incubation compared with the expression in the groups of polystyrene and smooth Ti supports the hypothesis that, after such geometry is sensed and considered to be favorable, cells create their own environment by secreting

the ECM proteins, and that, in a continuous feedback fashion[51] (Fig. 11). Our result in FN gene analysis corresponds, in part, with the results of two previous studies by Chou *et al.*[13,52] (1995 and 1996) from the Brunette group. In the first previous study, human gingival fibroblasts cultured on Ti reduced the FN mRNA level by 58% at 16 h, but increased it by 2.6-fold at 90 h compared to those on culture plastics, although the cell numbers on the two surfaces were essentially the same[52]. In our study, down-regulation of FN genes in the smooth Ti group compared to those in the control group at 24 h supports the above result. However, FN gene expression levels in the smooth Ti group were noted to be essentially the same with those in the polystyrene group at 48 and 72 h, or even reduced at 96 h. The reduction at 96 h seems to be due to the marked expression of FN gene in the polystyrene group compared with any other group on the same timeline. This result is in accordance with the other results of our study analyzing genes such as α5 integrin, cyclin E, CDK2, and CDK4. One possible explanation is that the fibroblasts in the polystyrene group were slower in reaching their confluence than the ones in the experimental groups. However, it still does not correspond with our viability and proliferation data that the fibroblasts in all groups, except those in TiD30, seems to have reached their confluence at 48 or 72 h. In the second previous study by Chou *et al.*[13] (1995), the authors compared the FN mRNA levels of fibroblasts cultured on smooth Ti and Ti with microgrooves of 3 µm in depth and 6-10 µm in width. In the study, the grooved surface increased the amounts of FN mRNA/cell approximately 3.5-fold at 16 hours, 1.9-fold at 40 hours and 2.2-fold at 90 hours. Despite the differences in microgroove dimensions, our result from the analysis on FN gene on successive timelines supports this previous result. It is confirmed that surface microgrooves of 15 and 30 µm in width and of equal 3.5 µm in depth on Ti substrata acted to up-regulate human gingival fibroblasts' FN gene on successive timelines from 24 to 72 h. However, due to the possibility of confluence at around 72 h of culture, the results at 96 h cannot be confirmed. After all, our data from the comparative analysis on FN gene

expression between the groups of various microgroove dimensions do not correspond with the result from the study by Chou *et al.*[13] (1995). Gene expression analysis at 96 h as well as at later phases needs further investigation.

As was mentioned earlier, cells align and stiffen ECM and partially unfold ECM proteins and, acting back, the ECM proteins reorganize the cytoskeleton of the cells. Integrins act to couple the two structures and, together with diverse intracellular signaling proteins recruited to the site, integrate signals in both inside-out and outside-in directions. Integrins recognize the outside-in signals such as positional cues encoded by the extracellular matrix and convert them into biochemical signals that control the cell's response to soluble growth factors and cytokines[53]. To analyze the cell-substratum adhesion of human gingival fibroblasts to the substrata used in this study, α5β1 integrin, a fibronectin receptor[54], has been analyzed in this study. Marked down-regulation of α5 integrin gene was noted in the groups of polystyrene and smooth Ti at 48 and 72 h of culture. Also, the gene was up-regulated in TiD15 and TiD30 at 24, 48, and 72 h (Fig. 11). The expression profile of α5 integrin gene in 20 samples on successive timelines coincided with that of FN gene, suggesting that human gingival fibroblasts in TiD15 and TiD30 were more active in FN assembly, namely the FN fibrillogenesis[55,56], than those in the groups of polystyrene and smooth Ti. Integrins can be localized in different adhesion structures called focal complexes, focal adhesions, fibrillar adhesions, and 3D-matrix adhesions. These structures reflect different stages of interaction between cells and ECM[57]. 3D-matrix adhesion was verified in a comprehensive study by Cukierman *et al.*[58] (2001). The joint up-regulation of FN and α5 integrin genes in TiD15 and TiD30 compared to the groups of polystyrene and smooth Ti suggests that human gingival fibroblasts cultured on Ti substrata with reasonably deep and wider microgrooves than the diameter of a single fibroblast actively formed either fibrillar adhesions or 3D-matrix adhesions,

or both, according to the criteria proposed by Cukierman *et al.*[58] (Fig. 12). Assuming that all the substrata induced formation of fibrillar adhesions due to the expression of α5 integrin gene in every sample regardless of the differences in degree, our result imply that fibroblasts in TiD15 and TiD30 might have been involved in forming 3D-matrix adhesions. However, β1 integrin genes showed even levels of expression in all groups on all timelines, except in the groups of polystyrene and smooth Ti at 72 h. This result requires evaluation of more molecules involved in adhesion structures, such as β3 integrin, paxillin, and focal adhesion kinase (FAK). After all, β1 integrin is known to be involved in diverse *in vivo* biology[59].

| Molecule | Focal adhesion (mature) | Fibrillar adhesion | 3D-matrix adhesion |
|---|---|---|---|
| $\alpha_5$ integrin | − p | + | + |
| $\beta_1$ integrin | + | + | + |
| $\beta_3$ integrin | + | − | − |
| paxillin | + | − | + |
| tensin | + | + | + |
| talin | + | + | + |
| vinculin | + | − | + |
| phospho-tyrosine | + | − | + |
| FAK | + | − | + |
| phospho-FAK [$Y^{397}$] | + | − | − |

Fig. 12. Molecular composition of three types of cell adhesions.

Cyclin D1 associates with cyclin-dependent kinases (CDKs) 4 and 6 to phosphorylate the retinoblastoma protein (pRb), blocks its growth inhibitory activity, and promotes the release of bound E2F transcription factor[60]. As a result, cyclin E–CDK2 and cyclin A–CDK2 complexes are activated, leading to the entry into and completion of S phase[61,62]. To evaluate the effect of substratum surface topography on G1/S cell cycle progression, we analyzed the expression of cyclin D1, E, and A2 genes as well as CDK4, 6, and 2 genes. The expression patterns of cyclin E, CDK4, and CDK2 genes coincided with those of FN and α5 integrin. However, cyclin D1 and cyclin

A2 genes showed exactly inverse expression profiles with those of cyclin E, CDK4, and CDK2 genes. The tendency was even true with the comparison between FN and α5 integrin genes (Fig. 11). It has previously been proposed that cyclin D1 in actively proliferating cells, whose elevated level is maintained through G1 phase but reduced in S phase and then elevated again in G2 phase for proliferation to continue, serves as a cell cycle regulatory switch[63]. In accordance to a view that cyclin D1 is inhibitory to DNA synthesis[64], the decline of cyclin D1 expression in S phase is not considered to be dependent on the environment of the cell, but directly regulated by cell cycle progression. DNA duplication occurs during S phase, which requires 10-12 hours and occupies about half of the cell-cycle time in most mammalian cells. A flattened morphology has been verified to be a prominent feature of S-phase cells and, in turn, the spread cells that are generally adhered to substratum are found during the S-phase[65,66]. Our result from the analyses on various cyclin- and CDK-genes is reminiscent of the fact that, in non-transformed cells, progression through cell cycle is tightly regulated on both translation and transcription levels. We suggest prudently that, referring to the viability and proliferation data in our study, human gingival fibroblasts on microgrooved and smooth Ti substrata were progressing through different stages of cell cycle at specific experiment time points, leading to the difference in the rate of reaching the confluence. We would like to point out that, so far, very little is known about the control of cell cycle progression after the cells have already started cycling. Since most of the cell cycle studies use serum-starved cultures, analysis on the steps involved in cell cycle progression from serum-deprived cultures is so rare[63]. Therefore, the results from our gene expression analyses on the molecules involved in cell cycle regulation cannot be directly applied to actively cycling cells due to the fact that all our experiments were basically done in serum-derived cultures. However, the fact that the complex nature of mammalian cell cycle regulation has not yet been fully uncovered still leaves a possibility that our results from gene analysis would yield a novel proposal,

assuming that more molecules be analyzed. For example, the gene expression data of cyclin D1 and cyclin A2 genes showing inverse expression profiles with those of FN gene, cyclin E gene, and so on, are the data that need research related to 3-D cell behavior. A study of gene expression profiling on vascular smooth muscle cells cultured in 3-D collagen matrices reported that a CDK inhibitor $p21^{cip1}$, known to have opposing regulatory functions to those of cyclin D1 in G1 phase cell cycle control, showed much higher gene expression level compared to the cells cultured on 2-D surfaces[67].

Regulation of α-SMA gene expression is a complex process and shows substantial tissue specificity[68]. Expression of α-SMA is one of the most reliable markers for myofibroblast differentiation and the prominent features of myofibroblasts are the development of a strong actin network reinforced by α-SMA and the presence of enhanced cell adhesion mechanisms[69]. TGF-β1 promotes the induction of the myofibroblastic phenotype through the activation of the RhoA–ROCK and JNK signaling pathways in human gingival fibroblasts. These phenotypical changes include the ability of cells to adhere and spread over fibronectin, the reinforcement of focal adhesion complexes, the organization of actin stress fibers, and the further induction of the myofibroblast marker α-SMA[70]. In our study, up-regulation of α-SMA gene in the polystyrene and smooth Ti group suggests that not only the tissue culture plastics but also the commercially pure titanium are capable of inducing myofibroblastic phenotype in human gingival fibroblasts, which was considered to be promoted by endogenous TGF-β1 or exogenous TGF-β1 in FBS. Down-regulation of α-SMA gene in TiD15 and TiD30 on all timelines in our study is in contrast to the result from Thampatty and Wang[71] (2007). In their study, human tendon fibroblasts cultured on the microgrooved surfaces increased α-SMA protein expression after treatment with TGF-β1. The authors suggested that TGF-β1 treated fibroblasts in microgrooves became differentiated into myofibroblasts. There are two

notable points to be discussed from their study. First, they did not compare the extent of α-SMA protein expression between the cells plated on smooth and microgrooved substrates. All the cells were plated only on microgrooved membranes and the group lacking in the TGF-β1 treatment was used as a control. Second, they used fibronectin-coated silicone membranes with surface microgrooves of 10 μm in groove and ridge width, and 3 μm in groove depth as culture substrata. The tendon fibroblasts showing extreme elongation appeared to be trapped inside the microgrooves, which might have affected the result. Since the microgrooves used in our study were greater in dimension compared to those used in the study by Thampatty and Wang, it may be inappropriate to compare the results of the two studies. The only similarity in the experimental designs lies in the fact that both studies used culture substrata with surface microgrooves. In addition, fibroblasts in both studies were treated with TGF-β1, since the growth factor was considered to be abundant in DMEM supplemented with 10% FBS used in all experiments in our study, whereas Thampatty and Wang incubated the cells in DMEM containing both 1% FBS and 5.0 ng/ml of TGF-β1 for 24 h. It has been postulated that growth response of human gingival fibroblasts to TGF-β1 or PDGF-BB stimulation in serum-free medium was equivalent to growth obtained in medium containing 10% FBS without added growth factors[72]. As verified in SEM, human gingival fibroblasts in our study were not observed to be trapped inside, but rather spontaneously crawled into the microgrooves. Therefore, we examined both TGF-βR-I and TGF-βR-II whose genes and proteins were verified in a previous study to show alterations in expression in relation to the change in fibroblasts' sensitivity to TGF-β1-induced α-SMA expression in 3-D environment compared to those in 2-D[73]. Although the authors used several types fibroblasts and a number of experimental designs, only their result from normal skin fibroblasts routinely cultured in supplemented DMEM containing 10% fetal calf serum without TGF-β1 treatment were compared with the result of our study. In their study, the result from Western blot analysis revealed that the fibroblasts in 3-D

culture expressed lower levels of α-SMA and TGF-βR-II but higher levels of TGF-βR-I compared to those cultured in 2-D monolayer culture. However, they used a unique 3-D culture system called 'spheroid culture', which lead the fibroblasts to differ in shape to that of the cells in TiD15 or TiD30 in our study. Presuming that the polystyrene/smooth Ti substrata and the microgrooved Ti substrata used in our study correspond to the 2-D and the 3-D environment used in the study by Kunz-Schughart *et al.*[73], respectively, the results from the two studies related to the α-SMA expression of the cultured cells correspond with each other. Likewise, the overall expression pattern of TGF-βR-II genes on all timelines in our study and the TGF-βR-II expression in the study by Kunz-Schughart *et al.*[73], both in relation to the α-SMA expression, correspond with each other except that the TGF-βR-II gene in TiD30 showed an inverse expression profile with that of the α-SMA gene (Fig. 13). This inverse gene expression profile was totally unexpected and strongly requires further investigation. It has been verified more than a decade ago that, unlike TGF-β1 with the ability to directly bind to TGF-βR-II, TGF-β2 binding to TGF-βR-II requires coexpression of TGF-βR-I[74], leading to an efficient formation of TGF-βR-I/R-II heteromer followed by activation of TGF-β1 signaling pathway. In our study, joint up-regulation of TGF-βR-I and TGF-βR-II was noted in TiD30 after 24 and 96 h of culture, while the α-SMA gene was down-regulated. Taken together, it is implied that titanium substrata with surface microgrooves of 30 μm in width and 3.5 μm in depth may act to trigger TGF-β1 signaling pathway. An interesting result from our study is an unexpected up-regulation of α-SMA gene in TiD60 after 72 h of culture. A recent study evaluating SMC behavior on 3-D microchannels in biodegradable polymeric films by Shen *et al.*[75] (2006) reported that the cells grown on flat film showed even expression of α-SMA after 3 days' and 7 days' culture, whereas the α-SMA expression of SMCs grown on 160 μm-wide and 25 μm-deep micropatterns was significantly enhanced after 7 days' culture compared to that after 3 days' culture. The

authors stated that the SMC phenotype shift from synthetic to a more contractile phenotype was observed when SMCs reached confluence on micropatterns with wide microchannels (80, 120, and 160 μm wide), in which the cells were found to proliferate with random orientation initially when the cell density was low, but switched to elongated morphology, unidirectional orientation, and a more contractile phenotype with increased α-SMA expression nearing confluence. The fibroblasts in TiD60 in our study might have undergone such process after descending into the microgrooves around at 72 h incubation. Also, joint up-regulation of cyclin D1 and cyclin A2 genes in TiD60 at 72 h incubation was noted along with an overall similarity in the gene expression pattern on all timelines to that of α-SMA gene (Fig. 13).

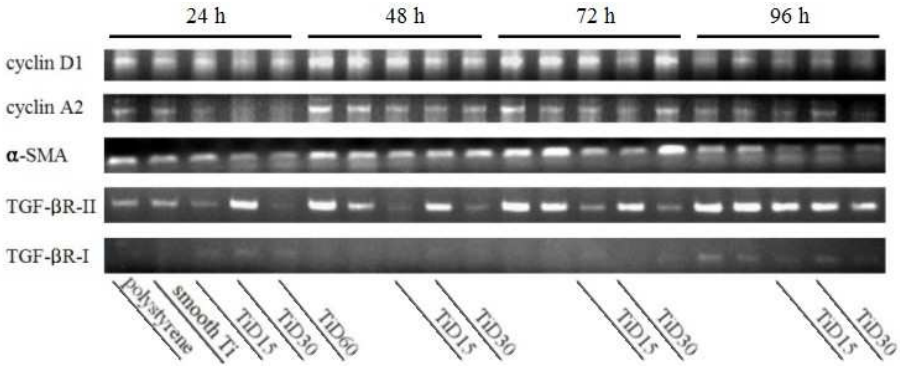


Fig. 13. Analysis on expression of genes encoding cyclin D1/A2, α-SMA, and TGF-βR-I/II.

Down-regulation of α-SMA gene was verified in another genomic analysis study on cells in 3-D matrix by Li *et al.*[67] In the study, the authors grew subcultured human aortic smooth muscle cells (HASMCs) in adherent collagen gels and compared the gene expression in 3-D matrix vs. that on 2-D matrix. For SMCs cultured in 3-D matrix; cells were cast into the collagen gel and for those cultured on 2-D matrix; cells were seeded on the top of the collagen gel. The authors reported the DNA microarray results that the expression of α-SMA in 3-D matrix was slightly lower than that in 2-D

matrix. They confirmed the result in RT-PCR as well as in Western blot analysis and concluded that both α-SMA gene and protein are down-regulated in 3-D collagen matrix compared to the 2-D matrix. Comparison of our RT-PCR results from the analyses on genes other than α-SMA with the results of the study by Li *et al.*[67] offers us a number of correspondences as well as several points to be discussed. The first gene to be compared is the p21 gene, also known as WAF1, p21CIP1, CDK-interaction protein 1, DNA synthesis inhibitor, and cyclin-dependent kinase inhibitor 1A. This gene encodes a potent cyclin-dependent kinase inhibitor. The encoded protein binds to and inhibits the activity of cyclin-CDK2 or -CDK4 complexes, and thus functions as a regulator of cell cycle progression at G1. The expression of this gene is tightly controlled by the tumor suppressor protein p53, through which this protein mediates the p53-dependent cell cycle G1 phase arrest in response to a variety of stress stimuli. This protein can interact with proliferating cell nuclear antigen (PCNA), a DNA polymerase accessory factor, and plays a regulatory role in S phase DNA replication and DNA damage repair. Li *et al.*[67] reported the significantly higher expression level of p21 gene in 3-D matrix by more than 2-fold increase compared with that in 2-D matrix and suggested that p21 may be responsible for the lower proliferation rate in 3-D matrix. In our study, relatively higher expression of p21 gene in primary human gingival fibroblasts was obvious in TiD30, and in a degree, in TiD60, compared with that in the groups of polystyrene, smooth Ti, and TiD15 after 24, 48, 72 h of culture. However at 96 h incubation, an inverse expression profile was noted with that on other timelines resulting in up-regulation of the gene in TiD15. This seems to be strongly related to the sudden decrease in the viability and proliferating activity of the fibroblasts in TiD15 at 96 h compared with those at 72 h, as has been confirmed by the XTT assay in this study. We suggested earlier that the result provides a strong implication of reaching the cells' confluence at around 72 h incubation. Also in mouse embryonic stem cells, p21 gene has been reported to be significantly up-regulated in 3-D porous tantalum

scaffold with the pore size up to 150 μm[76]. With our results from the analysis on α-SMA and p21 gene expression and with the results of the several studies discussed, we suggest that the fibroblasts on TiD30 in our study express specific genes that are characterized in 3-D matrix culture. Further, we confirmed this in SEM analysis on cellular morphology and conclude that, titanium substrata with surface microgrooves of 30 μm in width and 3.5 μm in depth provided human gingival fibroblasts with three-dimensional microenvironment. Indeed, Li *et al.*[67] characterized cell morphology by staining SMCs in 3-D or on 2-D collagen matrix on actin and vinculin, and found that the cells on 2-D matrix had prominent stress fibers and lamellipodia, whereas the cells in 3-D matrix had less actin stress fibers and usually had multiple filopodia that might follow the collagen fibrils due to contact guidance. We were able to verify this feature of cells in 3-D collagen matrix in TiD30 under SEM observations in our study. The second gene to be compared is cellular fibronectin (FN). Li *et al.*[67] postulated that higher expression levels of p21 and collagen I genes are the most prominent features in 3-D matrix culture compared with 2-D, which was again confirmed by Liu *et al.*[76] However, Li *et al.*[67] used collagen matrix for both 2-D and 3-D environment. Had it been the fibronectin matrix that they used for culture environment, their result would possibly have been a distinct one. In fact, in searching for clues for overcoming the failures for most biomaterials, Vogel and Baneyx[46] insisted upon using fibronectin matrix, not collagen. One of the reasons they proposed was that only fibronectin binds to α5β1 integrins and plays a central role in soliciting cellular behavior and integrin signaling that compares well to those found for cells in naturally occurring matrices. Following the view from Vogel and Baneyx[46], we analyzed expression of FN, α5 integrin, and β1 integrin genes and verified that FN genes were up-regulated and the expression was most pronounced in TiD30 at 24 and 48 h. In order to analyze the stimulatory effects of a 3-D microenvironment on cell-mediated fibronectin fibrillogenesis, Mao and Schwarzbauer[77] (2005) cultured fibroblasts on a pre-assembled 3D

fibronectin matrix and found significant stimulation of fibronectin fibril assembly compared to the cells in 2D culture. Again, the pronounced expression of FN and α5 integrin genes in TiD30 in our study suggests that titanium substrata with surface microgrooves of 30 μm in width and 3.5 μm in depth provided human gingival fibroblasts with three-dimensional context of culture and implies that the cells might have formed 3D-matrix adhesion. The third and the last gene to be compared is the cyclin A2 gene. Li *et al.*[67] assessed the SMCs' proliferation rate in 3-D or on 2-D matrices by subjecting the cells to flow cytometry analysis for DNA content after 24 h of culture and reported that SMCs in 3-D matrix had less cells in S phase than SMCs on 2-D matrix, but had more cells in G0/G1 phase, suggesting that SMCs in 3-D matrix had a lower proliferation rate. Indeed, they confirmed in microarray analysis that cyclin A1 gene was down-regulated in 3-D matrix, although expression of the gene is known to be specific to germ cells. Lower expression of cyclin A2 gene in TiD15, TiD30, and TiD60 at 24 h incubation compared with that in the groups of polystyrene and smooth Ti was noted in our study. Because Li *et al.*[67] did not continue to assess SMC proliferation at phases later than 24 h of culture, our result from the proliferation data using XTT assay on successive timelines were not compared with their result. Instead, we discuss here, further analysis on cyclin A2 gene at later phases of culture. The overall expression pattern of cyclin A2 gene corresponded with that of cyclin D1 gene on all timelines in our study. However, comparing the expression profiles of the two genes with that of p21 gene revealed that cyclin D1/A2 gene vs. p21 gene are inversely regulated, except in TiD15 at 48 h incubation and in all groups at 72 h incubation (Fig. 14). Assuming that the cells in different groups displayed varying proliferation rate, as has been confirmed in the timeline analysis with XTT assay, it is suggested that primary human gingival fibroblasts in our study underwent alterations in cell cycle progression and proliferation rate in a time period between 48 and 72 h of culture.

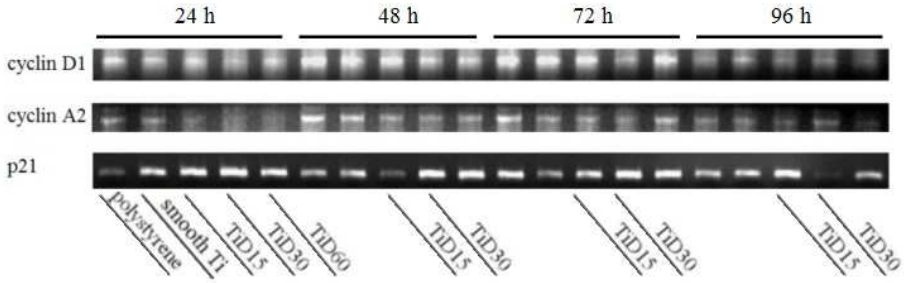

Fig. 14. Analysis on expression of genes encoding cyclin D1/A2 and $p21^{cip1}$.

To further confirm the complex regulation of the cell cycle genes, we analyzed gene expression of p27 and Skp2, the result of which merely aggravated the complexity. However, we found some of the interesting comparisons to be discussed. Comparison of the overall expression pattern of p27 gene with that of cyclin E gene revealed that the two genes showed a nearly exact inverse expression profile after 48, 72, and 96 of culture, except in TiD15 at 48 h, suggesting that p27 played a specific role in regulating the expression of cyclin E in human gingival fibroblasts cultured on titanium substrata with various dimensions of surface microgrooves (Fig. 15). Moreover, some of the results of marked p27 gene expressions even coincided with the expression profiles of cyclin D1/A2 genes. Among them, exclusion of the results of the marked p27 gene expression in the groups of polystyrene and smooth Ti leaves us the gene expression profiles under the two critical experimental conditions in our study, the TiD15 at 48 h and the TiD60 at 72 h. Pronounced expression of several genes under such conditions in this study strongly suggests that further analysis on additional genes be the key to unveiling the signal transduction pathways exclusive to sensing microgrooves. In addition to the reputed role in preventing the activation of cyclin E-CDK2 or cyclin D-CDK4 complexes, and thus controlling the cell cycle progression at G1, p27 has been reported to be involved in numerous other biological activities. Among them, a role has been suggested for cytoplasmic $p27^{kip1}$ in the regulation of cell migration independent of cyclin–CDK inhibition[78]. Also, p27 has even been suggested

to play a role in assembling and maintaining the stability of cyclin D1-CDK4 complexes[79]. It would be valuable to further establish the role of $p27^{kip1}$ in sensing the microenvironment, such as the microgrooves used in our study. Predominantly in S phase, activated $p27^{kip1}$ is specifically recognized by an F-box protein, S-phase kinase-associated protein-2 (Skp2 or p45). This protein interacts with S-phase kinase-associated protein 1 (SKP1 or p19) and, together with other F-box proteins constitutes one of the four subunits of ubiquitin protein ligase complexes called SCFs (SKP1-cullin-F-box). $SCF^{Skp2}$ is responsible for phosphorylation-dependent ubiquitination, that is the degradation, of $p27^{kip1}$. Recently, this Skp2 dependent-degradation of $p27^{kip1}$ has been verified to be regulated by focal adhesion kinase (FAK), thereby rendering the activity of Skp2 adhesion-dependent, while levels of $p21^{cip1}$ were regulated independent of Skp2[80]. We analyzed Skp2 gene and, again, the result merely aggravated the complexity in relation to the comparison with the p27 gene expression. However, on comparison between Skp2, NF-κB1, and TGF-βR-I genes, we found that the expression profiles of these genes almost exactly coincide with each other (Fig. 16). The genes were up-regulated in the groups of microgrooved Ti substrata at 24 and 96 h of culture, whereas nearly none of the three genes were readily expressed at 48 and 72 h of culture. The Rho GTPase, Rac1, has been shown to be an important downstream of Ras in cyclin D1 transcriptional regulation, and 3-D nanofibrillar surfaces have been suggested to induce sustained activation of Rac in NIH3T3 fibroblasts and normal rat kidney cells[81]. Also in mouse embryonic stem cells, enhanced proliferation and self-renewal of the cells on 3-D nanofibrillar surfaces have been shown to be correlated with the activation of Rac and phosphoinositide 3-kinase (PI3K) pathway. Since Rac1 induction of cyclin D1 transcription has been proposed to involve activation of a transcription regulator, NF-κB[82], we analyzed the expression of NF-κB1 in order to determine whether Rac-dependent signaling was involved in the induction of cyclin D1 transcription in fibroblasts cultured on microgrooved substrata. Comparing the expression profile of NF-κB1 gene with that of

cyclin D1 gene, we were not able to verify any relationship. Rather, the overall NF-κB1 gene expression was noted to show an inverse relationship with that of cyclin D1 gene and leaves much to be debated. Very recently, it was suggested that Rac-mediated induction of cyclin D1 mRNA requires activation of a parallel NF-κB pathway whereas ERK induces cyclin D1 transcription independent of NF-κB, implying that an NF-κB independent Rac signaling to the cyclin D1 gene exists[83].

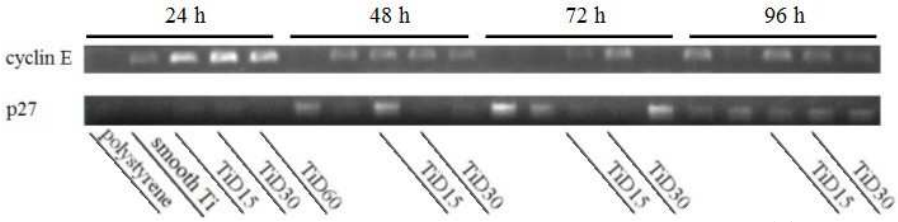


Fig. 15. Analysis on expression of genes encoding cyclin E and p21[cip1].

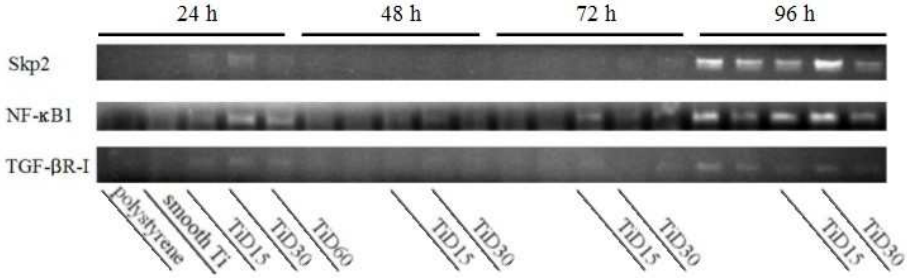


Fig. 16. Analysis on expression of genes encoding Skp2, NF-κB1, and TGF-βR-I.

One of very few studies with molecular analysis on the cells cultured on microgrooved substrata proposed an adhesion-mediated signal transduction involving FAK/Y397/Src-mediated ERK1/2 phosphorylation[84]. We believe that this proposal is a beginning of understanding the changes in cell behavior on microgrooved substrata in a molecular level. We also believe that further investigations on proliferation and cell cycle progression related to adhesion-mediated signaling associated with microgrooved substrata are on the way.

# V . CONCLUSION

In this study, we hypothesized that surface microgrooves of appropriate depth and extensive width on Ti substrata that enable the cells to readily descend into themselves, would alter various cell behaviors including viability and proliferation of cultured human gingival fibroblasts. The purpose of this study was to determine the dimension of surface microgrooves on Ti substrata that shows the greatest positive influence on characterizing specific cell behavior of cultured human gingival fibroblasts.

For this study, we prepared commercially pure titanium discs divided into four groups of smooth titanium substrata and the titanium substrata with surface microgrooves of monotonous 3.5 μm in depth and 15, 30, and 60 μm in width using photolithography. Adhesion, morphology, viability and proliferation, and gene expression of human gingival fibroblasts cultured on these substrata on successive timelines was analyzed and compared between groups. From the results, the following conclusions were made.

1. There was no difference between the numbers of human gingival fibroblasts adhered to smooth Ti substrata and those adhered to Ti substrata with surface microgrooves at 1 and 2 h incubation. Fibroblasts merely formed initial cell-substratum contact by the times.
2. In SEM, contact guidance of human gingival fibroblasts parallel to the direction of microgrooves was observed. Cells were able to readily descend into the microgrooves of 30 μm in width and 3.5 μm in depth at the early phase of culture, whereas at the later phase, cells in all groups were found both in the grooves and on the ridges. Cells on the ridge edges or in groove corners were spindle shaped with abundant filopodia formation towards the acid-etched surface

inside the microgrooves, thus mimicked the shape of the fibroblasts cultured in three-dimensional (3D) nanoenvironment.

3. On successive timelines, human gingival fibroblasts cultured on Ti substrata with various dimensions of surface microgrooves showed differences in the rate of reaching their confluence. Human gingival fibroblasts cultured on Ti substrata with microgrooves of 15 µm in width and 3.5 µm in depth significantly increased their viability and proliferation compared with those cultured on smooth Ti substrata after 72 h of culture and decreased after 96 h, whereas the cells on the microgrooves of 30 µm in width and 3.5 µm in depth continued increasing their viability and proliferation up to after 96 h of culture.
4. A joint up-regulation of matrix-assembly genes, such as fibronectin and α5 integrin genes, was noted in human gingival fibroblasts cultured on titanium substrata with microgrooves of 15 and 30 µm in width and an equal 3.5 µm in depth.
5. Gene expression pattern specific to the cells in 3D-matrix culture, such as down-regulation of α-smooth muscle actin gene along with up-regulation of fibronectin and p21 genes, was pronounced in human gingival fibroblasts cultured on Ti substrata with microgrooves of 30 µm in width and 3.5 µm in depth.

In reference to the results above, two conclusions were made.: 1) Surface microgrooves of 15 µm in width and 3.5 µm in depth on titanium substrata increase the viability and proliferation, as well as the expression of genes involved in the matrix assembly of cultured human gingival fibroblasts. 2) Surface microgrooves of 30 µm in width and 3.5 µm in depth on titanium substrata provide human gingival fibroblasts with a three-dimensional context of culture, thus show corresponding gene expression.

# VI . REFERENCES


1. Brunette, D. M. and Chehroudi, B.: The effects of the surface topography of micromachined titanium substrata on cell behavior in vitro and in vivo. *J. Biomech. Eng.* 121: 49-57, 1999.
2. Jansen, J. A., den Braber, E. T., Walboomers, X. F., and de Ruijter, J. E.: Soft tissue and epithelial models. *Adv. Dent. Res.* 13: 57-66, 1999.
3. Weiss, P.: Experiments on cell and axon orientation in vitro: the role of colloidal exudates in tissue organization. *J. Exp. Zool.* 100: 353–86, 1945.
4. den Braber, E. T., de Ruijter, J. E., Ginsel, L. A., von Recum, A. F., and Jansen, J. A.: Quantitative analysis of fibroblast morphology on microgrooved surfaces with various groove and ridge dimensions. *Biomater.* 17: 2037-44, 1996.
5. Wang, N., Ostuni, E., Whitesides, G. M., and Ingber, D. E.: Micropatterning tractional forces in living cells. *Cell Motil. Cytoskeleton* 52: 97-106, 2002.
6. Chen, C. S., Alonso, J. L., Ostuni, E., Whitesides, G. M., and Ingber, D. E.: Cell shape provides global control of focal adhesion assembly. *Biochem. Biophys. Res. Commun.* 307: 355-61, 2003.
7. Loesberg, W. A., Walboomers, X. F., van Loon, J. J., and Jansen, J. A.: The effect of combined cyclic mechanical stretching and microgrooved surface topography on the behavior of fibroblasts. *J. Biomed. Mater. Res. A* 75: 723-32, 2005.
8. Loesberg, W. A., Walboomers, X. F., van Loon, J. J., and Jansen, J. A.: The effect of combined hypergravity and micro-grooved surface topography on the behaviour of fibroblasts. *Cell Motil. Cytoskeleton* 63: 384-94, 2006.
9. Ingber, D. E.: Tensegrity II. How structural networks influence cellular information processing networks. *J. Cell Sci.* 116: 1397-1408, 2003.

10. Dalby, M. J.: Topographically induced direct cell mechanotransduction. *Med. Eng. Phys.* 27: 730-41, 2005.
11. Thery, M., Pepin, A., Dressaire, E., Chen, Y., and Bornens, M.: Cell distribution of stress fibres in response to the geometry of the adhesive environment. *Cell Motil. Cytoskeleton* 63: 341-55, 2006.
12. Folkman, J. and Moscona, A.: Role of cell shape in growth control. *Nature* 273: 345-49, 1978.
13. Chou, L., Firth, J. D., Uitto, V. J., and Brunette, D. M.: Substratum surface topography alters cell shape and regulates fibronectin mRNA level, mRNA stability, secretion and assembly in human fibroblasts. *J. Cell Sci.* 108: 1563-73, 1995.
14. Dalby, M. J., Riehle, M. O., Yarwood, S. J., Wilkinson, C. D., and Curtis, A. S.: Nucleus alignment and cell signaling in fibroblasts: response to a micro-grooved topography. *Exp. Cell Res.* 284: 274-82, 2003.
15. den Braber, E. T., de Ruijter, J. E., Smits, H. J., Ginsel, L. A., von Recum, A. F., and Jansen, J. A.: Quantitative analysis of cell proliferation and orientation on substrata with uniform parallel surface micro-grooves. *Biomater.* 17: 1093-99, 1996.
16. Walboomers, X. F., Croes, H. J., Ginsel, L. A., and Jansen, J. A.: Contact guidance of rat fibroblasts on various implant materials. *J. Biomed. Mater. Res.* 47: 204-12, 1999.
17. Walboomers, X. F., Monaghan, W., Curtis, A. S., and Jansen, J. A.: Attachment of fibroblasts on smooth and microgrooved polystyrene. *J. Biomed. Mater. Res.* 46: 212-20, 1999.
18. Chehroudi, B. and Brunette, D. M.: Subcutaneous microfabricated surfaces inhibit epithelial recession and promote long-term survival of percutaneous implants. *Biomater.* 23: 229-37, 2002.
19. Walboomers, X. F. and Jansen, J. A.: Effect of microtextured surfaces on the performance of percutaneous devices. *J. Biomed. Mater. Res. A* 74: 381-7, 2005.
20. Roehm, N. W., Rodgers, G. H., Hatfield, S. M., and Glasebrook, A. L.:

An improved colorimetric assay for cell proliferation and viability utilizing the tetrazolium salt XTT. *J. Immunol. Methods* 142: 257-65, 1991.

21. Zhang, C., Meng, X. F., Zhu, Z. H., Yang, X., and Deng, A. G.: Role of connective tissue growth factor in plasminogen activator inhibitor-1 and fibronectin expression induced by transforming growth factor β1 in renal tubular cells. *Chinese Med. J*. 117: 990-6, 2004.
22. Yao, M., Zhou, X. D., Zha, X. L., Shi, D. R., Jian Fu, J., He, Lu, H. F., and Tang, Z. Y.: Expression of the integrin α5 subunit and its mediated cell adhesion in hepatocellular carcinoma. *J. Cancer Res. Clin. Oncol.* 123: 435-40, 1997.
23. Bonson, S., Jeansonne, B. G., and Lallier, T. E.: Root-end Filling Materials Alter Fibroblast Differentiation. *J. Dent. Res.* 83: 408-13, 2004.
24. Shen, G., Xu, C. J., Chen, C., Hebbar, V., and Kong, A. N.: p53-independent G1 cell cycle arrest of human colon carcinoma cells HT-29 by sulforaphane is associated with induction of $p21^{CIP1}$ and inhibition of expression of cyclin D1. *Cancer Chemother. Pharmacol.* 57: 317–27, 2006.
25. Sawasaki, T., Shigemasa, K., Shiroyama, Y., Kusuda, T., Fujii, T., Parmley, T. H., O'Brien, T. J., and Ohama, K.: Cyclin E mRNA overexpression in epithelial ovarian cancers: inverse correlation with p53 protein accumulation. *J. Soc. Gynecol. Investig.* 8: 179-85, 2001.
26. Wong, H. and Riabowol, K.: Differential CDK-inhibitor gene expression in aging human diploid fibroblasts. *Exp. Gerontol.* 3: 311-25, 1996.
27. Mammoto, A., Huang, S., Moore, K., Oh, P., and Ingber D. E.: Role of RhoA, mDia, and ROCK in cell shape-dependent control of the Skp2-p27kip1 pathway and the G1/S transition. *J. Biol. Chem.* 279: 26323-30, 2004.
28. Baouz, S., Giron-Michel, J., Azzarone, B., Giuliani, M., Cagnoni, F., Olsson, S., Testi, R., Gabbiani, G., and Canonica, G. W.: Lung myofibroblasts as targets of salmeterol and fluticasone propionate:

inhibition of α-SMA and NF-κB. *Int. Immunol.* 17: 1473-81, 2005.

29. Boumédiene, K., Takigawa, M., and Pujol, J. P.: Cell density-dependent proliferative effects of transforming growth factor (TGF)-beta 1, beta 2, and beta 3 in human chondrosarcoma cells HCS-2/8 are associated with changes in the expression of TGF-beta receptor type I. *Cancer Invest.* 19: 475-86, 2001.
30. Okada, Y., Kato, M., Minakami, H., Inoue, Y., Morikawa, A., Otsuki, K., and Kimura, H.: Reduced expression of flice-inhibitory protein (FLIP) and NFkappaB is associated with death receptor-induced cell death in human aortic endothelial cells (HAECs). *Cytokine* 15: 66-74, 2001.
31. Grinnell, F., Ho, C. H., Tamariz, E., Lee, D. J., and Skuta, G.: Dendritic fibroblasts in three-dimensional collagen matrices. *Mol. Biol. Cell* 14: 384-95, 2003.
32. Walboomers, X. F., Ginsel, L. A., and Jansen, J. A.: Early spreading events of fibroblasts on microgrooved substrates. *J. Biomed. Mater. Res.* 51: 529–34, 2000.
33. Shen, M. and Horbett, T. A.: The effects of surface chemistry and absorbed proteins on monocyte/macrophage adhesion to chemically modified polystyrene surfaces. *J. Biomed. Mater. Res.* 57: 336-45, 2001.
34. Oakley, C., Jaeger, N. F., and Brunette, D. M.: Sensitivity of fibroblasts and their cytoskeletons to substratum topographies: Topographic guidance and topographic compensation by micromachined grooves of different dimensions. *Exp. Cell Res.* 234: 413-24, 1997.
35. Brunette, D. M. Fibroblasts on micromachined substrate orient hierarchically to grooves of different dimensions. *Exp. Cell Res.* 164: 11-26, 1986.
36. Jiang, G., Huang, A. H., Cai, Y., Tanase, M., and Sheetz, M. P.: Rigidity sensing at the leading edge through αvβ3 integrins and RPTPα. *Biophys. J.* 90: 1804-9, 2006.
37. Walboomers, X. F., Croes, H. J., Ginsel, L. A., and Jansen, J. A.: Growth behavior of fibroblasts on microgrooved polystyrene. *Biomater.* 19:

1861-8, 1998.

38. Tillman, J., Ullm, A., and Madihally, S. V.: Three-dimensional cell colonization in a sulfate rich environment. *Biomater.* 27: 5618–26, 2006.
39. Noh, H. K., Lee, S. W., Kim, J. M., Oh, J. E., Kim, K. H., Chung, C. P., Choi, S. C., Park, W. H., and Min, B. M.: Electrospinning of chitin nanofibers: degradation behavior and cellular response to normal human keratinocytes and fibroblasts. *Biomater.* 27: 3934-44, 2006.
40. Partridge, M. A. and Marcantonio, E. E.: Initiation of attachment and generation of mature focal adhesions by integrin-containing filopodia in cell spreading. *Mol. Biol. Cell* 17: 4237-48, 2006.
41. Galbraith, C. G., Yamada, K. M., and Galbraith, J. A.: Polymerizing actin fibers position integrins primed to probe for adhesion sites. *Science* 315: 992-5, 2007.
42. Kim, H., Murakami, H., Chehroudi, B., Textor, M., and Brunette, D. M.: Effects of surface topography on the connective tissue attachment to subcutaneous implants. *Int. J. Oral Maxillofac. Implants* 21: 354-65, 2006.
43. Bottaro, D. P., Liebmann-Vinson, A., and Heidaran, M. A.: Molecular signaling in bioengineered tissue microenvironments. *Ann. N. Y. Acad. Sci*. 961: 143-53, 2002.
44. Kaiser, J. P., Reinmann, A., and Bruinink, A.: The effect of topographic characteristics on cell migration velocity. *Biomater.* 27: 5230-41, 2006.
45. Sun, F., Casse, D., van Kan, J. A., Ge, R., and Watt, F.: Geometric control of fibroblast growth on proton beam-micromachined scaffolds. *Tissue Eng*. 10: 267-72, 2004.
46. Alaerts, J. A., De Cupere, V. M., Moser, S., van den Bosh de Aguilar, P., and Rouxhet, P. G.: Surface characterization of poly(methyl methacrylate) microgrooved for contact guidance of mammalian cells. *Biomater.* 22: 1635-42, 2001.
47. den Braber, E. T., de Ruijter, J. E., Ginsel, L. A., von Recum, A. F., and Jansen, J. A.: Orientation of ECM protein deposition, fibroblast

cytoskeleton, and attachment complex components on silicone microgrooved surfaces. *J. Biomed. Mater. Res.* 40**:** 291–300, 1998.

48. Thery, M., Racine, V., Pepin, A., Piel, M., Chen, Y., Sibarita, J. B., and Bornens, M.: The extracellular matrix guides the orientation of the cell division axis. *Nat. Cell Biol.* 7: 947-53, 2005.
49. Chen, C. S., Mrksich, M., Huang, S., Whitesides, G. M., and Ingber, D. E.: Geometric control of cell life and death. *Science* 276:1425-28, 1997.
50. Vogel, V. and Baneyx, G.: The tissue engineering puzzle: A molecular perspective. *Ann. Rev. Biomed. Eng.* 5: 441-63, 2003.
51. Vogel, V.: Mechanotransduction involving multimodular proteins: converting force into biochemical signals. *Annu. Rev. Biophys. Biomol. Struct.* 35: 459-88, 2006.
52. Chou, L., Firth, J. D., Nathanson, D., Uitto, V. J., and Brunette, D. M.: Effects of titanium on transcriptional and post-transcriptional regulation of fibronectin in human fibroblasts. *J. Biomed. Mater. Res.* 31: 209-17, 1996.
53. Giancotti, F. G. and Tarone, G.: Positional control of cell fate through joint integrin/receptor protein kinase signaling. *Annu. Rev. Cell. Dev. Biol.* 19: 173-206, 2003.
54. Mould, A. P., Askari, J. A., Aota, S., Yamada, K. M., Irie, A., Takada, Y., Mardon, H. J., and Humphries, M. J.: Defining the topology of integrin α5β1-fibronectin interactions using inhibitory anti-α5 and anti-β1 monoclonal antibodies. *J. Biol. Chem.* 272: 17283-92, 1997.
55. Pankov, R., Cukierman, E., Katz, B. Z., Matsumoto, K., Lin, D. C., Lin, S., Hahn, C., and Yamada, K. M.: Integrin dynamics and matrix assembly: tensin-dependent translocation of α5β1 integrins promotes early fibronectin fibrillogenesis. *J. Cell Biol.* 148: 1075-90, 2000.
56. Clark, K., Pankov, R., Travis, M. A., Askari, J. A., Mould, A. P., Craig, S. E., Newham, P., Yamada, K. M., Humphries, and M. J.: A specific α5β1 integrin conformation promotes directional integrin translocation and fibronectin matrix formation. *J. Cell Sci.* 118: 291-300, 2005.

57. Zaidel-Bar, R., Cohen, M., Addadi, L., and Geiger, B.: Hierarchical assembly of cell–matrix adhesion complexes. *Biochem. Soc. Transact.* 32: 416-20, 2004.
58. Cukierman, E., Pankov, R., Stevens, D. R., and Yamada, K. M.: Taking cell-matrix adhesions to the third dimension. *Science* 294: 1708–12, 2001.
59. Brakebusch, C. and Fassler, R.: β1 integrin function in vivo: adhesion, migration and more. *Cancer Metastasis Rev.* 24: 403-11, 2005.
60. Sherr, C. J. and Roberts, J. M.: CDK inhibitors: positive and negative regulators of G1-phase progression. *Genes Dev.* 13: 1501-12, 1999.
61. Girard, F., Strausfeld, U., Fernandez, A., and Lam, N. C.: Cyclin A is required for the onset of DNA replication in mammalian fibroblasts. *Cell* 67: 1169-79, 1991.
62. Weinberg, R. A.: The retinoblastoma protein and cell cycle control. *Cell* 81: 323– 30, 1995.
63. Stacey, D. W.: Cyclin D1 serves as a cell cycle regulatory switch in actively proliferating cells. *Curr. Opin. Cell Biol.* 15: 158-63, 2003.
64. Pagano, M., Theodoras, A. M., Tam, S. W., Draetta, G. F., and Chen, J.: Cyclin D1-mediated inhibition of repair and replicative DNA synthesis in human fibroblasts. *Genes Dev.* 8: 1627-39, 1994.
65. Ingber, D. E., Prusty, D., Sun, Z., Betensky, H., and Wang, N.: Cell shape, cytoskeletal mechanics, and cell cycle control in angiogenesis. *J. Biomech.* 28: 1471–84, 1995.
66. Meredith, D. O., Owen, G. R., ap Gwynn, I., and Richards, R. G.: Variation in cell-substratum adhesion in relation to cell cycle phases. *Exp. Cell Res.* 293: 58-67, 2004.
67. Li, S., Lao, J., Chen, B. P., Li, Y. S., Zhao, Y., Chu, J., Chen, K. D., Tsou, T. C., Peck, K., and Chien, S.: Genomic analysis of smooth muscle cells in 3-dimensional collagen matrix. *FASEB J.* 17: 1376, 2003.
68. Mack, C. P., Somlyo, A. V., Hautmann, M., Somlyo, A. P., and Owens, G. K.: Smooth muscle actin differentiation marker gene expression is

regulated by RhoA-mediated actin polymerization. *J. Biol. Chem.* 276: 341–347, 2001.

69. Tomasek, J. J., Gabbiani, G., Hinz, B., Chaponnier, C., and Brown, R. A.: Myofibroblasts and mechano-regulation of connective tissue remodelling. *Nat. Rev. Mol. Cell Biol.* 3: 349–363, 2002.
70. Smith, P. C., Cáceres, M., and Martinez, J.: Induction of the myofibroblastic phenotype in human gingival fibroblasts by transforming growth factor-beta1: role of RhoA-ROCK and c-Jun N-terminal kinase signaling pathways. *J. Periodontal Res.* 41: 418-25, 2006.
71. Thampatty, B. P. and Wang, J. H.: A new approach to study fibroblast migration. *Cell Motil. Cytoskeleton* 64: 1-5, 2007.
72. Anderson, T. J., Lapp, C. A., Billman, M. A., and Schuster, G. S.: Effects of transforming growth factor-beta and platelet-derived growth factor on human gingival fibroblasts grown in serum-containing and serum-free medium. *J. Clin. Periodontol.* 25: 48-55, 1998.
73. Kunz-Schughart, L. A., Wenninger, S., Neumeier, T., Seidl, P., and Knuechel, R.: Three-dimensional tissue structure affects sensitivity of fibroblasts to TGF-beta 1. *Am. J. Physiol. Cell Physiol.* 284: C209-19, 2003.
74. Rodriguez, C., Chen, F., Weinberg, R. A., and Lodish, H. F.: Cooperative binding of transforming growth factor (TGF)-β2 to the types I and II TGF-β receptors. *J. Biol. Chem.* 270: 15919-22, 1995.
75. Shen, J. Y., Chan-Park, M. B., He, B., Zhu, A. P., Zhu, X., Beuerman, R. W., Yang, E. B., Chen, W., and Chan, V.: Three-dimensional microchannels in biodegradable polymeric films for control orientation and phenotype of vascular smooth muscle cells. *Tissue Eng.* 12: 2229-40, 2006.
76. Liu, H., Lin, J., and Roy, K.: Effect of 3D scaffold and dynamic culture condition on the global gene expression profile of mouse embryonic stem cells. *Biomater.* 27: 5978-89, 2006.

77. Mao, Y. and Schwarzbauer, J. E.: Stimulatory effects of a three-dimensional microenvironment on cell-mediated fibronectin fibrillogenesis. *J. Cell Sci.* 118: 4427-36, 2005.
78. Assoian, R. K.: Stopping and going with $p27^{kip1}$. *Dev. Cell* 6: 458-9, 2004.
79. Bagui, T. K., Mohapatra, S., Haura, E., and Pledger, W. J.: $P27^{kip1}$ and $p21^{Cip1}$ are not required for the formation of active D cyclin-cdk4 complexes. *Mol. Cell Biol.* 23: 7285–90, 2003.
80. Bryant, P., Zheng, Q., and Pumiglia, K.: Focal adhesion kinase controls cellular levels of p27/Kip1 and p21/Cip1 through Skp2-dependent and -independent mechanisms. *Mol. Cell Biol.* 26: 4201-13, 2006.
81. Nur-E-Kamal, A., Ahmed, I., Kamal, J., Schindler, M., and Meiners, S. Three dimensional nanofibrillar surfaces induce activation of Rac. *Biochem. Biophys. Res. Commun.* 331: 428-34, 2005.
82. Boyer, L., Travaglione, S., Falzano, L., Gauthier, N. C., Popoff, M. R., Lemichez, E., Fiorentini, C., and Fabbri A.: Rac GTPase instructs NF-κB activation by conveying the SCF complex and IκB-α to the ruffling membranes. *Mol. Biol. Cell* 15: 1124-33, 2004.
83. Klein, E. A., Yang, C., Kazanietz, M. G., and Assoian, R. K.: NFkappaB-independent signaling to the cyclin D1 gene by Rac. *Cell Cycle* 6: 1115-21, 2007.
84. Hamilton, D. W. and Brunette, D. M.: The effect of substratum topography on osteoblast adhesion mediated signal transduction and phosphorylation. *Biomater.* 28: 1806-19, 2007.

# 국문 요약

## 표면 마이크로그루브의 크기가 티타늄 기판 상에서 배양된 인간치은섬유아세포의 세포행동에 미치는 영향

연세대학교 대학원 치의학과 (지도교수 이 근 우)

이 석 원

치과용 티타늄 임플란트와 주위 연조직간의 반응을 증진시킬 것으로 기대되는 티타늄 표면 마이크로그루브가 실제 세포행동에 미치는 영향을 규명하려는 노력이 전개되고 있다. 이러한 연구들에서 널리 사용된 마이크로그루브들은 대부분 배양된 세포의 직경보다 작은 1-10μm의 폭을 가지며 섬유아세포의 형태 변화를 야기하여 focal adhesion의 형성을 증가시키고 유전자 발현에 영향을 주는 것으로 알려져 있으나, 실험실 내 세포 증식이나 동물 생체 내 epithelial down-growth에 대한 영향은 아직까지 규명되지 못하였다.

본 연구에서는 단일 세포가 안착될 수 있는 충분한 폭과 깊이를 가지는 마이크로그루브가 섬유아세포의 세포행동, 특히 세포생존력 및 증식을 증진시킨다는 가설을 제시하였고, 이의 평가를 위하여 다양한 크기의 표면 마이크로그루브가 부여된 티타늄 기판 상에서 배양된 인간치은섬유아세포의 세포부착, 세포형태, 세포생존력 및 증식, 유전자 발현 등에 대한 분석을 시행하였다. 본 연구의 목적은 티타늄 기판 상에서 배양된 인간치은섬유아세포의 세포행동을 특징 지움에 있어 가장 바람직하게 영향을 줄 수 있는 표면 마이크로그루브의 크기를 규명하고자 하였다.

포토리토그래피를 이용하여 순수 티타늄 표면에 폭과 깊이가 각각 15/3.5 μm, 30/3.5 μm, 60/3.5 μm인 마이크로그루브를 부여하고 실험군으로 (TiD15, TiD30, TiD60), 평활한 티타늄 기판을 대조군으로 사용하였다 (smooth Ti). 각 기판 표면에서 인간치은섬유아세포를 24, 48, 72, 96시간 동안 각각 배양하고 크리스탈 바이올렛 염색, XTT분석, 주사전자현미경관찰, reverse transcriptase-polymerase chain reaction 등을 통하여 그루브의 유무와 크기에 따른 세포의 부착, 형태, 생존력 및 증식, 유전자 발현 등의 차이를 분석하였다. 세포부착과 생존력 및 증식의 경우 일요인 분산분석을 이용하여 통계 분석을 시행하였다.

이상 4가지 분석의 결과는 다음과 같다.

1. 세포부착 분석 결과 티타늄 기판 상에서 배양된 인간치은섬유아세포는 표면 마이크로그루브 유무와 크기에 따른 유의차를 보이지 않았다. 세포 접종 1시간 및 2시간 후 인간치은섬유아세포는 초기 세포-기판 접촉만을 형성하였다.
2. 세포형태 분석 결과 표면 마이크로그루브가 부여된 티타늄 기판 상에서 배양된 인간치은섬유아세포는 그루브의 방향과 평행하게 contact guidance를 나타내었다. 30/3.5μm 폭/깊이의 그루브는 배양 후기뿐 아니라 초기에도 그루브 내로 세포를 안착시킬 수 있었다. 능선의 모서리나 그루브의 코너에 위치한 섬유아세포들은 왕성한 filopodia의 형성 등 삼차원 배양 시와 유사한 세포형태를 나타내었다.
3. 세포생존력 및 증식의 배양시간에 따른 분석 결과 티타늄 기판 상에서 배양된 인간치은섬유아세포는 표면 마이크로그루브의 크기에 따라 세포 포화 속도에 차이를 보였다. 인간치은섬유아세포는 15/3.5μm 폭/깊이의 마이크로그루브에서 72시간 배양 시 평활한 티타늄 기판에 비하여 유의한 증가를 보였으나 96시간에서 급격한 감소를 나타낸 반면, 30/3.5μm 폭/깊이의 마이크로그루브에서는 96시간까지 지속적이고 점진적인 증가를 나타내었다.
4. 15/3.5μm 및 30/3.5μm 폭/깊이의 마이크로그루브에서 배양된 인간치은섬유아세포는 fibronectin과 α5 integrin 등 기질단백질의 생성과 관계된 유전자 발현의 동반 증가를 나타내었다.
5. 30/3.5μm 폭/깊이의 마이크로그루브 상에서 배양된 인간치은섬유아세포는 α-smooth muscle actin 유전자 발현의 감소와 더불어 fibronectin 및 p21 유전자 발현의 증가 등 3차원 세포배양 시 특징적인 유전자 발현의 양상을 나타내었다.

이상의 결과에 따라 티타늄 기판 표면 15/3.5μm 폭/깊이의 마이크로그루브는 배양된 인간치은섬유아세포의 세포생존력 및 증식을 증진시키고 기질단백질 생성 유전자들의 발현을 증진시키며, 30/3.5μm 폭/깊이의 마이크로그루브는 인간치은섬유아세포에게 3차원 세포배양의 환경을 제공하여 상응하는 세포형태와 유전자 발현을 유도하는 것으로 결론지을 수 있다.

---

핵심 되는 말: 티타늄, 마이크로그루브, 섬유아세포, 세포증식, 유전자발현